An unusual 'shovel-billed' dinosaur with trophic specialisations from the early Campanian of Trans-Pecos Texas and the ancestral hadrosaurian crest

Albert Prieto-Márquez[1,2]*, Jonathan R. Wagner[3] and Thomas Lehman[3]

[1]Institut Català de Paleontologia Miquel Crusafont, Universitat Autònoma de Barcelona, Sabadell, Barcelona, Spain; [2]Museu de la Conca Dellà-Parc Cretaci, Isona, Lleida, Spain; [3]Departament of Geosciences, Texas Tech University, Lubbock, TX 79409†

*Corresponding author. Email: albert.prieto@icp.cat

†Current address: 603 Prickly Pear Pass, Buda, TX, 78610

We describe a new genus and species of hadrosaurid dinosaur, *Aquilarhinus palimentus*, from the lower shale member of the Aguja Formation (lower Campanian) of Big Bend National Park, southwestern Texas. This species is characterized by several autapomorphies of the facial skeleton and mandible, including a crest composed of broadly arched nasals. Notably, the symphyseal processes of the dentary are elongated and reflected dorsally, causing the dentaries to meet with a w-shaped anterior profile. A hypothesized shovel-shaped 'bill,' associated with widening of the skull, in *A. palimentus* might have been used in shoveling out and scooping up semiaquatic vegetation. This animal is otherwise superficially similar to kritosaurins like *Gryposaurus* but differs in retention of key plesiomorphic character states in the maxilla and jugal.

Phylogenetic analysis reveals *Aquilarhinus* to be a non-saurolophid hadrosaurid allied to *Latirhinus* from the late Campanian of Mexico, which bears a similar broadly-arched nasal. The recognition of this lineage adds to the diversity of non-saurolophid hadrosaurids and points to the existence of a hitherto unknown diversity of 'duck-billed' dinosaurs outside of the saurolophine-lambeosaurine radiation. Cranial crests were ancestral for early hadrosaurids and evolved before the saurolophid radiation. Ancestrally, crests were 'solid,' and consisted of arched nasals. These were retained among kritosaurins and subsequently modified into the diverse crest morphologies observed among derived saurolophines. Lambeosaurine 'hollow-crested' crest morphology departed from the ancestral, 'solid-crested' pre-saurolophid condition early following the onset of that clade.

Keywords: Dinosauria; Hadrosauridae; phylogeny; evolution; Cretaceous; North America

Introduction

Hadrosaurid dinosaurs are among the most diverse components of the North American Late Cretaceous terrestrial vertebrate fauna, particularly during the middle to late Campanian (Ostrom 1961; Prieto-Márquez 2010a,b; Gates *et al*. 2012; Freedman Fowler & Horner 2015). These animals are unique in possessing a combination of complex dental batteries (Erickson *et al*. 2012), a reconfiguration of their facial skeleton to accommodate hypertrophied nasal passages (Wagner 2004; Evans 2006), and a wide variety of solid and hollow supracranial crests (Ostrom 1962; Hopson 1975; Evans *et al*. 2009). Although much is known of the later evolution of hadrosaurids during the acme of their diversity in North America during the middle-late Campanian (Lull & Wright 1942; Horner *et al*. 2004; Lund & Gates 2006), comparatively little is known of the evolution of hadrosaurids during the preceding Santonian through early Campanian. This is mainly due to the sparseness of the fossil record from that interval, although the rarity of non-saurolophid hadrosaurids from later times also limits inference about ancestral character states.

The Aguja Formation of western Texas preserves one of the southernmost Campanian terrestrial vertebrate faunas in North America. Nearly the entire fauna, however, is known from the uppermost part of the formation – the upper shale member of Lehman (1985; reviewed by Rowe *et al*. 1992; Cifelli 1994; Sankey 2001; Lehman & Busbey 2007). Until recently, very little was known about the vertebrate fauna found in the lower part of the formation (the lower shale member). Wick *et al*. (2015) and Brink (2016) described a diverse assemblage of small theropod, lizard, and mammal teeth (the 'Lowerverse local fauna') from a single locality in the lower shale

member, and Lehman *et al*. (2019) describe the fauna and stratigraphy of the lower shale member in general, but otherwise the vertebrate fossils of the lower Aguja Formation remain undocumented.

We here describe a new species of hadrosaurid dinosaur from the lower shale member, the first of several reports intended to document the larger terrestrial vertebrates from these strata. The holotype specimen of this new hadrosaurid (TMM 42452-1) was briefly described previously by Wagner (2001; see also Wagner & Lehman 2001) and at that time referred to *Kritosaurus* sp. nov. Subsequent study of the specimen, however, indicates that the new species cannot be included within *Kritosaurus*, and differs sufficiently from other hadrosaurids such that it warrants recognition as the holotype of a new genus and species.

The vertebrate fauna from the lower shale member dates back between 81 and 80 Ma, corresponding to the early Campanian (see below). This fauna may be slightly older than that of the Wahweap Formation in Utah and lower Two Medicine Formation in Montana (Wick *et al*. 2015; Brink 2016, Lehman et al., 2019). Only a few hadrosaurids have been described from these strata, such as *Gryposaurus latidens* (Prieto-Marquez 2012) and *Acristavus gagslarsoni* (Gates *et al*. 2011), and these are among the oldest known hadrosaurids. The new species from the lower shale member is therefore significant in adding to our understanding of the early evolution and diversity of the clade. In particular, this animal is uniquely positioned, both phylogenetically and temporally, to expand our understanding of the early evolution of hadrosaurid supracranial ornamentation.

Institutional abbreviations

AMNH: American Museum of Natural History, New York, USA; **IGM**: Museo de Paleontología, Instituto de Geología, Universidad National Autónoma de México, México D.F., México; **MOR**: Museum of the Rockies, Bozeman, Montana, USA; **NMMNH**: New Mexico Museum of Natural History and Science, Albuquerque, New Mexico, USA; **ROM**, Royal Ontario Museum, Toronto, Canada; **TMM**: Texas Vertebrate Paleontology Collections, The University of Texas at Austin, Austin, Texas, USA.

Geological Setting

Terrestrial and paralic strata of the Aguja Formation are widely exposed in and around Big Bend National Park in southwestern Texas. These strata are underlain by and intertongue with marine deposits of the Pen Formation. The Aguja consists of two eastward-thinning intervals of terrestrial strata (the lower and upper shale members) separated by a westward-thinning wedge of interposed marine strata - the McKinney Springs tongue of the Pen Formation (Fig. 1). The upper shale member is widely exposed throughout Big Bend National Park and surrounding areas, but the lower shale member is mostly exposed on private ranches west of the Park; it thins and pinches out in the southwestern part of the Park and does not extend into the eastern portion.

The lower shale member of the Aguja Formation consists primarily of thick beds of lignitic clayshale with several prominent sandstone and coal beds, particularly near the base. In the middle of the lower shale member there is a thin zone of interbedded very fine sandstone and carbonaceous mudstone with conspicuous iron-manganese concretions. This concretionary interval is the only part of the lower shale member that yields significant vertebrate fossils and the holotype specimen of the new hadrosaurid here documented was collected from these strata.

Lehman (1985) interpreted the lower shale member as having accumulated primarily in a coastal swamp or marsh environment. Wagner (2001) provided a detailed taphonomic and facies interpretation of the type locality of the new taxon here described. The specimen was recovered from within a bed of mudstone having irregular bedding planes covered with abundant large carbonized leaf and wood fragments, many of which are riddled with *Teredolites* borings. The bones are partially enclosed in large concretions of iron-manganese oxides. Some of the bones were broken prior to burial, but articulation surfaces are intact and the cortical surfaces exhibit little cracking, indicating that the bones had been subject to minimal transport or weathering prior to burial. Immediately overlying the bone-bearing bed is a thin layer with abundant small ostreid bivalve shells, but no other remains are preserved at the site.

The deposit represents a single burial, with the preserved elements somewhat channelized along an approximate east-west axis, and preserves many easily winnowed elements. The left manus, parts of at least one pes, and parts of the skull and cervical series were preserved along with parts of the pelvis. The manus and part of the skull of the specimen were somewhat disarticulated and held in place by concretionary material. Carbonized plant debris, abundant in the surrounding sediments, was found intimately intermixed with the skull and manus; these elements may have become entangled in vegetation, retarding transport.

The over-representation of easily transportable elements and the absence of regions of the skeleton consisting of elements more difficult to transport (e.g., long bones of the appendicular skeleton) suggest that this may be an allochthonous deposit, with the preserved material having moved some distance downstream from where the body first was first entrained. It is possible, however, that elements from unrepresented skeletal regions were present at the site but concealed beneath the overburden and were simply not found. Alternately, it is possible that the carcass

was scavenged prior to burial and that dispersed the skeleton. However, the hydrodynamic similarity and apparent channelized distribution of the elements suggest that hydrodynamic sorting was a significant factor in the generation of the deposit.

The bone-bearing horizon lies at the base of gently inclined heterolithic strata . The association of small oysters and *Teredolites* with the site attests to the presence of brackish conditions, The rhythmic lithological heterogeneity of the immediately overlying deposits supports a paralic, tidally influenced environment. The inclination of the bedding is likely due to lateral migration of a small stream. This and the disarticulated, slightly winnowed, and apparently current-aligned nature of the specimen support the hypothesis that it was deposited on the bed of a shallow tidal creek and subsequently covered by point bar deposits.

Systematic paleontology

Dinosauria Owen, 1842

Ornithischia Seeley, 1887

Ornithopoda Marsh, 1881

Iguanodontia Dollo, 1888

Hadrosauridae Cope, 1870 (sensu Prieto-Márquez, 2010a)

Aquilarhinus gen. nov.

Type species. *Aquilarhinus palimentus* sp. nov.

Etimology. From the Latin ‘aquila’, meaning ‘eagle’, and the Greek ‘rhinos’, meaning ‘nose’. The combination of these two words references the morphology of the rostrum.

Diagnosis. As for the type and only known species.

Aquilarhinus palimentus sp. nov.

Kritosaurus sp. nov. Wagner, 2001; Wagner and Lehman, 2001.

Etimology. The specific name is a combination of the Latin words ‘pala’, shovel, and ‘mentus’, chin, in reference to the assumed resemblance of the predentary to a spade or shovel given the dorsomedial projection of the symphyseal process of the dentary.

Holotype and only known specimen. TMM 42452-1, represented by a sphenoid fragment, both nasals, right maxilla, right jugal, right quadratojugal, partial left and right palatines, partial right dentary, partial first ceratobranchial, partial neural arch of atlas, fragments of two cervical centra, two cervical ribs, partial sacral rib, left carpal, nearly complete left manus, postacetabular process of right ilium, fragment of right ischium, partial astragali, pedal phalanx III-1, and four pedal unguals. Most parts of TMM 42452-1 were collected in 1983 by T. Lehman, N. LaFon, and K. Davies. In 1999, J. Wagner and T. Lehman continued excavation of the site collecting additional elements. The preserved parts of the skull and jaws were disarticulated but closely associated. All of these bones were found within four square meters and clearly represent a single individual.

Diagnosis. Hadrosaurid dinosaur possessing the following autapomorphies: nasals transversely broad across skull table; premaxillary shelf of maxilla at anterior apex flat and as broad as proximal segment of palatal process; palatine extending nearly horizontally to contact maxilla; dorsally reflected symphysial process of dentary. Differs from other hadrosaurids in possessing maxilla combining jugal process and ectopterygoid ridge continuous with ventral margin of jugal facet. Differs from all other hadrosaurids except *Latirhinus uitstlani* in nasal enclosing extremely broad and subcircular lateral profile of external bony naris.

Occurrence. The type locality is on the western flank of Rattlesnake Mountain, in early Campanian strata of the lower shale member of the Aguja Formation, southwestern corner of Big Bend National Park, Brewster County, southwestern Texas (USA) (Fig. 1).

Ages for the terrestrial deposits in the upper and lower shale members are constrained by ammonite biostratigraphy for underlying and overlying marine strata,and a few radiometric age determinations. The uppermost biostratigraphically significant ammonite found in the Pen Formation below the Aguja is *Scaphites hippocrepis* III (Waggoner 2006), which occurs in a zone having an estimated age of c. 81 Ma (Gradstein *et al*. 2012). *Baculites haresi* is found in paralic strata (the Rattlesnake Mountain and Terlingua Creek sandstone members) in the Aguja Formation above the lower shale member (Waggoner 2006). This ammonite is known to range in the western United States as high as the *Baculites obtusu*s zone, which includes a tuff with an age of 80.97 Ma (Ogg *et al*. 2012). The uppermost part of the upper shale member includes intercalated pyroclastic deposits that yield U/Pb ages ranging from c. 77 Ma (Befus *et al*. 2008) to c. 73 Ma (Breyer *et al*. 2007). The vertebrate fauna of the upper shale member has been

collected almost exclusively from levels below the pyroclastic deposits, and so must have an age between 80 and 77 Ma (middle Campanian). The vertebrate fauna from the lower shale member is older, between 81 and 80 Ma (early Campanian).

Osteology of *Aquilarhinus palimentus*

Skull and mandible

In general aspect, the skull as reconstructed was almost certainly tall and would have had a steeply-sloping facial profile, as in *Gryposaurus* (Gates & Sampson 2007; Figure 2). As noted below, there is circumstantial evidence to indicate that the skull roof sloped anteroventrally, and the external bony naris was exceedingly large. A remarkable departure from the generally narrow saurolophine aspect of this species is a general mediolateral expansion of the skull. This is evidenced by the broad exposure of the nasal on the skull roof, the shallow angle of inflection of the palatine vault, and the mediolateral extent of the symphysial process of the dentary. This expansion is here interpreted as dilation of the skull mediolaterally about the midline, resulting in greater separation of paired cranial elements. Dilation of the cranium appears to be a morphogenetic accommodation to the modification of the anterior dentary (below).

With reconstructed quadrate and skull lengths of 26 cm and 57 cm, respectively, TMM 42452-1 is a relatively small individual for a hadrosaurid. For example, compared to other hadrosaurids of the same time period, the skull of TMM 42452-1 is estimated to be only 50% the length of the holotype skull of *Gryposaurus latidens* (Horner 1992; Prieto-Márquez 2012), and 65% of the length of the type skulls of *Acristavus gagslarsoni* (Gates *et al*. 2011) and

Probrachylophosaurus bergei (Freedman Fowler & Horner 2015). By analogy with *Gryposaurus* spp. (Prieto-Márquez 2010c), it could be assumed that the nasal arch of *Aquilarhinus palimentus* would become more prominent with growth. However, it is also possible that the nasal arch of *A. palimentus* experienced a different allometric growth trajectory than *Gryposaurus* spp. Therefore, we are uncertain at this juncture regarding the degree of maturity of TMM 42452-1 pending the discovery of additional specimens.

Nasal. Both nasals are nearly completely preserved in TMM 42452-1, missing only the distal ends of the supranarial processes and fragments of the posterodorsal and posterolateral margins (Figs. 3 and 4). Both elements show evidence of plastic and brittle distortion. The nasals have been flattened, warping the dorsal and lateral surfaces into the same plane, and the base of the supranarial process of the right nasal has been broken and displaced approximately 20 degrees anteromedially (Fig. 4). An irremovable ferruginous concretion coats the surfaces of both nasals.

The central region of the nasal forms a broad plate. The dorsal portion of the nasal would be horizontal in life, while the lateral region formed a significant part of the side of the skull. Although distorted in both nasals, the dorsal surface appears to be approximately parallel to the dorsal margin of the premaxillary articulation when viewed laterally. Given the angulation of the premaxillary articulation with the maxilla, this practically requires that the dorsal margin of the skull sloped anteroventrally, at least at the level of the nasals. This is comparable with the elevation of the posterior region of the skull in *Gryposaurus* (Gates and Sampson 2007; Prieto-Márquez 2010c) and *Kritosaurus* (Prieto-Márquez 2014), but because of the tenuous nature of this conclusion and the extent of plastic deformation in the specimen we have left the relevant

character (192 in our list, Supplemental online material 1) coded as uncertain for *Aquilarhinus palimentus* in our character-taxon matrix (Supplemental online material 2).

The supranarial process is shallow and extends anteriorly, as well as somewhat dorsally, from the body of the nasal, arching broadly over the external bony naris (Fig. 3). In lateral view, this arch closely resembles that of *Gryposaurus* spp. (Gates and Sampson 2007, Prieto-Márquez 2012) and, particularly, *Latirhinus uitstlani* (Prieto-Márquez and Serrano-Brañas 2012). In *Aquilarhinus palimentus*, however, the nasal arch extends farther anteriorly and is more broadly curved than in *Gryposaurus*. Three-dimensionally, the nasal arch of *A. palimentus* appears to be mediolaterally thicker, with the supranarial processes together forming a hollow arch at its base, rather than the flattened, appressed, plate-like nasals and mediolaterally compressed supranarial processes of *Gryposaurus* (Prieto-Márquez 2010c). This is in accord with the mediolateral dilation of the skull noted above. Each supranarial process gradually tapers anteriorly and features a gentle scallop in its dorsal profile where the processes divide to embrace the ascending process of the premaxilla. No articular facet for the supranarial process of the premaxilla is clearly demarcated on either nasal. The left nasal preserves a sigmoid curve in dorsal view that, if not due entirely to post-mortem distortion, suggests that the premaxilla flared widely anteriorly between the supranarial processes.

The nasal meets its counterpart over the external bony naris at a thickened, obliquely striated medial sutural facet (Fig. 3). The dorsal surface of the nasal arch is smooth, unlike the rugose surfaces of some specimens of *Gryposaurus notabilis* (Prieto-Marquez, 2010c) and *Naashoibitosaurus ostromi* (Prieto-Márquez 2014, fig 21) or *Rhinorex* (Gates and Scheetz 2015).

The great dorsoventral breadth of the narial margin on the nasal indicates an exceedingly large external bony narial foramen, as in *Latirhinus uitstlani* (Prieto-Márquez and Serrano

Brañas 2012). The circumnarial fossa is shallow and poorly emarginated, as in brachylophosaurins (Horner 1983; Prieto-Márquez 2005; Freedman-Fowler and Horner 2015) and *Gryposaurus* spp. (Gates and Sampson 2007; Prieto-Márquez 2010c). The circumnarial fossa clearly intersects the facet for the premaxilla on the lateral face of both nasals, at which point the fossa is relatively broad. The fossa must therefore have excavated the lateral process of the premaxilla as typically occurs in hadrosaurids (Prieto-Márquez 2010a). Indeed there is a converse bulge on the intracranial surface of the left nasal for the circumnarial fossa where it crosses the region of the premaxillary facet (Fig. 3B).

The triangular ventral process of the nasal posteroventrally underlies the external narial foramen (Fig 3B). At the anteroventral vertex of this process there is a narrow, shallow facet for reception of the lateral process of the premaxilla. Posterior to the ventral process, the posteroventral margin of the nasal body thins, presumably for its insertion into the dorsal articular slot of the lacrimal (Fig. 4B, C); a thin, arcuate flat surface dorsal to the edge of the bone marks the region where the lacrimal contacts the nasal. The posterior margin of the nasal body, above the lacrimal articulation, features a trapezoidal surface for articulation with the prefrontal (Fig. 4B, C). This surface features a pair of slightly raised ridges that would have been parallel to the descending process of the prefrontal. Further dorsally, the posterodorsal end of the main body of the nasal meets the frontal. Although both nasals have been somewhat crushed and deformed flat, it seems clear that the posterior portion of the skull table was subhorizontal (possibly anteroventrally inclined), and the base of the nasal arch presents a marked anterodorsal inflection of the skull table, not a gentle dorsal arch rising smoothly from the skull roof.

Maxilla. The maxilla is rectangular in lateral view, straight in dorsal view and slightly sigmoidal in ventral view (Fig. 5). It is broadly convex laterally and flattened medially in anterior view, The alveolar margin is roughly straight. Along the margin are 40 alveoli surrounded by very thin bone. At the anterior end of the bone, the anterior maxillary apex ('anteroventral process' of others; Fig. 6B) forms a 30-degree angle with the alveolar margin. The dorsolateral surface of this apex forms a shelf for supporting the lateral process of the premaxilla (Fig. 5A, B). Unlike other hadrosaurids like *Brachylophosaurus* (e.g., MOR 1071-8-5-99-447N), *Naashoibitosaurus* NMMNH P-16106), *Edmontosaurus* (e.g., MOR 1609), or *Prosaurolophus* (e.g., MOR 447-8-7-1-86), the anterior end of the premaxillary shelf is not concave, nor is it emarginated from the lateral wall of the maxilla by a distinct lip; it is nearly flush with the surface of the anterior maxilla, but forms an extensive smooth articular surface in lateral view (Fig. 5A). The shelf is separated by a subtle round ridge anteroventrally where it laterally contacts the two most proximal alveoli.

Above the maxillary apex, an extremely thin, almost sheet-like, palatal process ('anterodorsal process' of others) juts anteromedially from the anterodorsal corner of the body of the maxilla. Although the pendant portion of the process is missing, given the moderate slope of the dorsal margin of the anterior maxilla, it is likely that the palatal process was less angled anteroventrally than in *Gryposaurus* (e.g., MOR 553). The dorsal surface of the palatal process encloses a shallow groove that extends posteriorly and blends into a prominent shelf medial to the dorsal process of the maxilla, marking the maxillary margin of the osseous choana (choanal shelf, Fig. 6A, B).

Posterodorsal to the premaxillary shelf and posterior to the palatal process there is the enlarged round maxillary foramen that is characteristic of hadrosauroids (homologized by

Weishampel [1984] with the antorbital fenestra). As in saurolophine hadrosaurids (Prieto-Márquez 2010a), this foramen opens anterolaterally onto the anterodorsal margin of the maxilla, where it is typically partly or completely obscured by the overlying lateral process of the premaxilla. This enlarged anterior foramen is the anterior extension of the path for the maxillary neurovascular package, a bundle that passes anteriorly (in an anteriodorsal arc in hadrosaurids) into the maxilla through a gap between the jugal and palatine processes at the anterior end of the ectopterygoid shelf. The enclosing osseous tunnel sends branching channels to form the prominent peribuccal series of foramina of most iguanodonts, extending along the lateral surface of the maxilla from the first posterior-most foramen just anterior to the juncture of the ectopterygoid shelf and the jugal facet to the enlarged anteriormost foramen just discussed (Davies 1983).

The dorsal process rises as an equilateral triangle that is wider than tall. It extends from the dorsal margin of the central region of the maxilla. The anterodorsal portion of the dorsal process forms a flange bearing a textured lateral surface that is contacted by the lacrimal (Fig. 5A, B). The articular surface of this lacrimal flange is convex posteroventrally and extends to the midline of the dorsal process. Adjacent and ventral to the lacrimal facet, the articular surface for the jugal occupies the remainder of the lateral surface of the dorsal process of the maxilla. The articular facet for the jugal extends further ventrally and posteriorly beyond the dorsal process on the lateral surface of the maxilla, overall mirroring the arrow-shaped contour of the anterior process of the jugal.

The thicker posterior margin of the dorsal process wraps medially around itself and is anteriorly inclined, as in non-hadrosaurid hadrosauroids (e.g., *Gilmoreosaurus mongoliensis* AMNH FARB 30653), brachylophosaurins (e.g., *Probrachylophosaurus bergei*, MOR 2919),

and *Naashoibitosarus ostromi* (NMMNH P-16106). The anterior portion of the anterior process of the jugal wraps around this surface toward its contact with the palatine, roofing a small foramen between the dorsal process and the palatine process of the maxilla as well as the palatine. This 5 mm wide foramen (homologized with the antorbital fenestra by Horner [1992]) opens out onto the previously mentioned choanal shelf medial to the dorsal process, where smaller foramen passes ventrally from the choanal shelf medial to the dorsal process ventrally to the maxillary neurovascular passage.

Notably, unlike other hadrosaurids except *Eotrachodon orientalis* (Prieto-Márquez *et al*. 2016a) and as in non-hadroaurid hadrosauroids (e.g., *Gilmoreosaurus mongoliensis,* Prieto-Márquez & Norell [2010]) and non-hadrosauroid iguanodontians (e.g., *Iguanodon bernissartensis*, Norman [1980]), there is a jugal process projecting posteriorly and slightly laterally from the jugal articular surface. We hypothesize that in other hadrosaurids this process became reduced to a tubercle (i.e., the 'dorsal jugal tubercle' of Wagner, 2001; Wagner and Lehman, 2009). Anteroventral to the jugal process, the ventral border of the articular surface for the jugal extends laterally forming a prominence with a flattened surface. This surface (the 'ventral jugal tubercle' of Wagner, 2001; Wagner and Lehman, 2009; Fig. 5A, B) is a prominence or facet for articulation with the ventral spur of the anterior process of the jugal. Below this facet, the roughly textured anterior end of the ectopterygoid ridge roofs the medial margin of the coronoid fossa (Fig. 5A, B). As in all hadrosaurids, except *Eotrachodon* (Prieto-Márquez *et al*. 2016a), the ectopterygoid shelf is fully continuous with the ventral margin of the jugal articular surface. The line of peribuccal maxillary foramena passes in a shallow arc, concave dorsally, from the enlarged anteriormost foramen to a point immediately anterior to the coronoid fossa where the enlarged, posterior-most foramen represents the first anteroventral

branch of the maxillary neurovascular package after it enters the maxilla proper, as in other hadrosaurids. Two more significant foramina penetrate the lateral maxilla anterior to this, and two much smaller foramina continue the row anteriorly to the enlarged anteriormost foramen. This row is only slightly dorsally arched, not curved around the jugal articulation as in most saurolophids, and is, like the ectopterygoid shelf, set much higher on the wall of the maxilla than in non-hadrosaurid hadrosaurs.

Posterior to the choanal shelf and medial to the dorsal process, a low palatine ridge rises from the medial margin of the maxilla (Fig. 6A, B). The articular face for the palatine is directed dorsally but has been abraded such that its limit can be only barely discerned. Continuing posteriorly along the dorsal outline of the palatine ridge, and barely produced above the ectopterygoid shelf, is the base of the abraded pterygoid process.

The posterior portion of the maxillary body is occupied by a broad and ventrolaterally inclined ectopterygoid shelf (Fig. 5C, D). Unlike non-hadrosaurid hadrosauroids (Prieto-Márquez 2010a) and the non-saurolophid hadrosaurid *Eotrachodon* (Prieto-Márquez *et al*. 2016b), but as in other hadrosaurids, the ectopterygoid shelf of *Aquilarhinus* accounts for over 35% of the length of the maxilla. The ectopterygoid ridge, the lateral margin of the ectopterygoid shelf, forms a thick lip overhanging the coronoid fossa. However, unlike other hadrosaurids but as in *Eotrachodon*, the ectopterygoid ridge of *Aquilarhinus* is steeply inclined posteroventrally, forming an angle of 18 degrees with the tooth row in lateral view.

The medial surface of the maxilla bears an arcuate row (concave ventrally) of 40 alveolar foramina passing along the dorsal margin of the maxillary body, the “special” foramina of Edmund (1957) through which buddings of the dental lamina likely passed into the alveolar files to form teeth. Below this row of foramina extends the relatively smooth dental parapet (Norman

1980). Its ventral margin exhibits a shallow groove orientated parallel to the ventral margin of the maxilla, the "vascular groove" observed by Lambe (1920) in *Edmontosaurus*.

Jugal. The jugal of *Aquilarhinus palimentus* is a triradiate, boomerang-shaped plate, with a nearly straight ventral margin extending between the anterior process and the posteroventral flange (Fig. 7). In dorsal view, the bone is straight but with an abrupt inflection at the midpoint of the orbit where the jugal curves medially to join the maxilla to form the anterior limit of the coronoid fossa.

The anterior process is relatively shallow and forms an elongate, arrow-shaped flange in lateral view. The apex of the anterior process is missing its distal tip but it was probably relatively long, as the preserved segment is already over half the length of the main body of the anterior process. As in non-brachylophosaurin saurolophines (Prieto-Márquez 2010a), the ventral spur of the anterior process is well offset posteriorly relative to the level of the summit of dorsal (lacrimal) margin of the process. The ventral spur is triangular and wider than it is deep. Most of the roughly textured medial surface of the anterior jugal articulates with the maxilla, posterolaterally embracing the jugal process ('dorsal jugal tubercle') and spreading anteriorly and ventrally from that point. The maxillary articular facet on the medial jugal is bounded posteriorly by a subvertical, sharp and prominent ridge, and the triangular surface articulation for the maxilla anterior to this ridge is further divided into a dorsal and ventral portion by a horizontal ridge (Fig. 7C, D). Dorsal to the posterior ridge the edge of the jugal forms a joint with the palatine. This elongate facet is slightly offset medially relative to the maxillary facet, and extends obliquely (anterodorsally) as in *Eotrachodon orientalis* (Prieto-Márquez *et al*.

2016a) and *Lophorhothon atopus* (Langston 1960). The dorsal margin of the anterior process of the jugal meets the ventral margin of the (unpreserved) lacrimal.

The postorbital process projects nearly perpendicularly from the long axis of the jugal, between the lacrimal margin of the anterior process and the quadratojugal flange, separating the U-shaped margins for the orbit and infratemporal fenestra (Fig. 7A, B). The process is V-shaped in cross-section, its longitudinal axis is twisted somewhat medially along its lower half and the process rises more dorsally in the distal half. The open side of the 'V' is orientated anteriorly and somewhat medially, with a longer lateral flange. The medial flange is incomplete, but it is clear that both together formed a gently expanding groove which was deepest two-thirds of the way up the process for the reception of the jugal process of the postorbital. Near the end of the process, both flanges and the groove between them sweep posteriorly to form a rounded tip.

The infratemporal margin is slightly narrower than the orbital border and the infratemporal bar is 1.5 times deeper than the orbital constriction. A tongue-shaped posteroventral flange extends from beneath the infratemporal margin. The ventral expansion of the posteroventral flange is rather limited, being only 1.3 times deeper than the infratemporal bar. The quadratojugal flange appears to be expanded posteriorly, with posteriorly-divergent anterodorsal and posteroventral margins, as in *Eotrachodon orientalis* (Prieto-Márquez *et al*. 2016a) and brachylophosaurin hadrosaurids (Horner 1983; Prieto-Márquez 2005; Freedman Fowler & Horner 2015). The bone is thicker along the dorsal (infratemporal) margin, and thins posteriorly and ventrally. On the medial surface of the flange, partially obscured by matrix, there is an extremely shallow subtrapezoidal facet for the lap joint with the anterior portion of the quadratojugal. The posteroventrally concave posterior margin of the jugal between the posteroventral and quadratojugal flanges forms a relatively broad arc.

Quadratojugal. The quadratojugal is a relatively small subtriangular lamina that thickens posteriorly (Fig. 7E–H). The anteroventral, or free, margin is concave anteroventrally, curving gently from the quadratojugal facet of the quadrate to the quadratojugal process of the jugal. The anterodorsal edge is straight and orientated anteroventrally, but angles abruptly ventrally a short distance above the anteroventral border to form a squared off anterior terminus. This border is extremely thin, particularly dorsally. The posterior margin of the quadratojugal is thin and rounded, and curves somewhat medially around a dorsoventral axis through the quadrate facet. The ventral apex is not preserved.

The medial side of the quadratojugal is slightly concave due to the medial curvature of the posterior margin. Along the posterior margin of the bone there is a raised surface for articulation with the quadrate. This surface is divided into two oval concavities by a gap. This gap may occupy a position homologous to the quadratojugal portion of the paraquadratic foramen in non-hadrosaurid iguanodontians (Norman 1980; Head 1998). The medial surface of the quadratojugal is ornamented by fine striations that converge on the central depression.

The lateral surface of the quadratojugal is covered by acute and pronounced striations, which converge on a point just anterior to the center of the posterior margin of the element. Anteriorly, the lateral surface of the quadratojugal is dominated by a broad, shallow facet for the jugal. This facet has very subtle, rounded posterior and posteroventral margins. The ventral margin of the jugal facet is produced laterally as a small lip that embraces the jugal ventrally and almost laterally. The structure of this lip is such that the jugal is free to move, in nearly any direction except ventrally relative to the quadratojugal

Palatine. Although incomplete, both palatines of TMM 42452-1 were recovered. The palatine consists of two major regions: a medially directed shaft and a plate that lies against the palatine ridge of the maxilla (Fig. 8). The plate of the palatine is mostly missing, owing to its delicate lamellar nature. The preserved proximal remnant of the plate is V-shaped in cross-section. The medial portion is orientated vertically and articulates with the dorsomedial edge of the palatine process of the maxilla, whereas the lateral part is orientated ventrolaterally and wraps around the lateral edge of the palatine process of the maxilla. The lateral portion of the plate is thickened toward the junction with its counterpart. At that junction, the plate forms a medial ridge on its exposed surface. It is against this ridge that the palatine process of the pterygoid articulates.

The medial process of the palatine sweeps anteromedially from the maxilla as a thin pillar with an airfoil-shaped cross-section. Although most illustrations of the hadrosaurid palate show the palatine being steeply inclined dorsally (e.g., Heaton 1972, fig. 5), in TMM 42452-1 the palatine extends nearly directly medially with only a slight dorsal inclination (Fig. 8). The posterior edge of the process, with the ridge for articulation with the pterygoid, twists dorsally as the leading and trailing edges diverge medially and the shaft itself thins. The resulting medial end, for articulation with the vomer, pterygoid, and the other palatine, is a thin edge directed nearly horizontally, rather than subvertically as in other hadrosaurids.

Anteromedially, the edge of the medial process of the palatine thickens over a short distance laterally, then diverges into two ridges separated by a shallow fossa. The ventralmost of these ridges proceeds ventrally along the midline of the shaft, expanding to form the shoe-shaped anterior end of the articulation with the palatine process of the maxilla. The dorsal of these ridges forms the leading edge of the medial process. The lateral edge of the bone is expanded as an

airfoil-shaped vertically striated articular facet for the jugal and possibly part of the dorsal process of the maxilla.

Sphenoid. The braincase of TMM 42452-1 is solely represented by the sphenoid (Fig. 9). It consists of the central body of the element, missing the rostrum and all but the bases of both basipterygoid processes . Much of the surficial bone has been weathered, with the outer lamellae of cortical bone exfoliated. The anteroventral surface is preserved, framed by the bases of the basipterygoid processes. This surface exhibits a well-developed median ridge along the posterior half, presumed to be homologous with the ventromedian process of the basisphenoid noted by Gates and Sampson (2007). The angle between the basipterygoid processes cannot be measured.

The posterodorsal basioccipital articulation is chevron-shaped, with the peak directed anterodorsally. Each 'arm' of the chevron is deeply striated, with the striae extending anterodorsomedially to meet at a sagittal groove. These 'arms' would have articulated posteriorly with the basal tubera. The alar process typical of hadrosaurids is not preserved. The distal termini of the 'arms' form the bases of two stout, dorsally arched pillars extending anteriorly. A deep fossa lies between theses pillars as in other hadrosaurids, and the fractured bases of the basipterygoid processes projected anteroventrolaterally from them.

A shallow flange occupies the centre of the preserved right lateral surface, extending dorsoanteromedially before angling abruptly anteriorly. Between this flange and the body of the bone passes the vidian canal for the anterior portions of the internal

carotid artery and the vidian branch of cranial nerve VII. The medial margin of the left vidian canal is also preserved, and the two canals converge anterodorsally but do not meet in the preserved portion of the bone. These would have remained separate as in many reptiles, passing via paired foramina anterorodorsally through the dorsum sella into the sella turcica (neither of which is preserved). It is unclear if the vidian canals were partly or completely roofed over by bone, or if they remained open posterodorsally for their entire length.

Dentary. The right dentary of TMM 42452-1 preserves much of the mandibular ramus, including the symphysial region to the middle of the ramus and a fragment of its posterior extent, as well as a portion of the coronoid process (Fig. 10). Overall, the dentary of this specimen is typically hadrosaurian, but with a dramatically different symphysial architecture.

The preserved mandibular ramus includes at least 18 tooth positions. With two to three positions missing from the anterior end of the tooth row and a small number of alveoli represented on unattached fragments, there must have been at least two dozen or more tooth positions. The mandibular ramus is subelliptical in cross section and mediolaterally compressed. On the medial face of the mandibular ramus there is a shallow Meckelian groove underlying the dental battery. Anteriorly, the ventral margin of the dentary is deflected ventrally forming a 19-degree angle with the long axis of the tooth row. The edentulous portion of the dorsal margin of the dentary is short relative to other hadrosaurids. Specifically, the proximal edentulous slope of the dentary is only as long as the combined width of four or five teeth.

The symphysial process is airfoil shaped in cross-section, with the surface of greatest curvature orientated ventrally. This process is unique in *Aquilarhinus palimentus* in being

dorsally recurved (Fig. 10B), in addition to the anteromedial orientation shared with other hadrosaurids (Prieto-Márquez 2010a) (Fig. 10J). The symphyseal process of TMM 42452-1 is angled anteromedially and dorsally such that its ventral surface is inclined 55 degrees relative to the lateral wall of the mandibular ramus when viewed anteriorly (Fig. 10B). The dorsal orientation is exaggerated by slight crushing but by not more than five degrees at most. The symphysial groove is orientated in line with the process, such that the grooves they met an obtuse angle medially in anterior view. The two mandibles in articulation would form a W-shape in anterior view. This is distinct from the situation in all other hadrosaurids, in which the symphysial process is angled slightly medioventrally, and the symphyses meet almost horizontally in articulated specimens, forming a U-shaped anterior end of the mandible (Lull and Wright 1942). A row of four small foramina is set in a shallow arc around the anterior edge of the base of the symphysial process (Fig. 9B). These foramina are all orientated toward the articulation with the predentary.

As in other iguanodontians (Norman 1980), the inner wall of the alveolar chamber is formed by the dentary parapet, a thin lamellum of bone which is absent in TMM 42452-1, exposing the tooth battery in medial view. Along the ventromedial edge of the chamber, where the lateroventral wall of the chamber and the dentary parapet join, is a row of small foramina that is concave dorsally in medial view as it follows the ventral profile of the alveolar chamber. This region is badly abraded in the specimen, making it impossible to determine the morphology of these foramina, but they are likely the 'special foramina' of Edmund (1957).

A fragment of the coronoid process is present, missing the bulk of the shaft but preserving part of the apex. The dorsal region of the coronoid process appears to be broadly rounded and expanded in the sagittal plane of the mandible, more so anteriorly than posteriorly

as in saurolophid hadrosaurids (Prieto-Márquez 2010a). Posteriorly, it bears a slot-like articulation for the ascending process of the surangular. This slot-like articulation gradually closes towards the apex of the coronoid process.

Hyoid apparatus. A first ceratobranchial, probably the left, is preserved with TMM 42452-1 (Fig. 10D, E). The preserved portion consists of a laterally compressed shaft with a moderately expanded head. The shaft is slightly convex dorsally, and almost imperceptibly convex medially about a dorsoventral axis. It is oval in cross-section and laterally compressed posteriorly, and anteriorly becomes more D-shaped (convex laterally) before it expands into the head, which forms a rounded rectangle in cross-section. At mid-length of the shaft, a lateral swelling exhibiting a rugose texture may represent a muscle attachment surface. The anterior head is incompletely preserved ventrally but shows a modest expansion. Although descriptions of hadrosaur hyoids are rare (e.g., Ostrom 1961; Head 1998; Gates *et al*. 2007), this bone appear to be particularly reduced in *Aquilarhinus*.

Dentition. Most details of the enamelled side of maxillary teeth are obscured by the intact walls of the maxillary alveolar chamber (Fig. 6E). Overall, the teeth are largest beneath the anterior end of the coronoid fossa and become smaller posteriorly and more so anteriorly. The occlusal surface is angled at approximately 30-40 degrees from the apparent parasagittal section of the bone. Each maxillary alveolus harbours a single functional tooth, unlike in saurolophines where it is typical for at least some positions to bear at least two functional teeth. In some positions the worn root of the preceding tooth is still present lateral to its functional successor, but the crown has been lost to abrasion and there is still only one functional tooth. The crowns of the teeth are

enameled only on the labial side, as in all hadrosaurid maxillary teeth (Horner *et al*. 2004). Each enamelled face bears a strong median ridge; on the teeth of the posterior quarter of the maxilla, the ridge is set increasingly distally. Marginal denticles are hardly discernible: they appear to be greatly reduced, if not absent on all maxillary (and dentary) teeth.

The dentary teeth are poorly preserved (Fig. 10G). Although no more than two teeth may be seen in any particular tooth file, there is enough space in most alveolar grooves for at least three fully formed teeth (as in saurolophids). Damage to the occlusal margin of the toothrow is extensive. However, at least one tooth file has two functional teeth exposed on the occlusal plane (again as in saurolophids), and the thickest portion of the dentary (where the most functional teeth per file would be expected) was not recovered. The crowns of the teeth are only enameled on the lingual side, as in other hadrosaurids. The enameled face of the crown is roughly diamond-shaped, with a prominent median ridge. The poor preservation of these crowns prevented assessing the presence and shape of marginal denticles. The length to width ratio of the most complete crown is 2.4. Crown-root angles could not be measured, but appear to be relatively low, in the range commonly given for saurolophine hadrosaurids (Sternberg 1936; Horner 1992; Weishampel *et al*. 1993). Each tooth is slightly overlapped by the tapering dorsal halves of the successional crowns in the neighbouring rows. The size distribution of the preserved teeth suggest that the largest examples were in the unrecovered central section of the dentary.

Axial skeleton

Cervical vertebrae. The atlas is solely known from the nearly complete left side of the neural arch of TMM 42452-1. It consists of a stout base topped by a prominent, plate-like spine inflected dorsomedially about the longitudinal axis of the vertebral series. A prominent dorsomedial inflection is present above the base of the neural arch. Slightly below this inflection, along the anterior margin of the arch, is a thickened area supporting a subcircular anteromedially-facing articular facet, presumably for reception of the occipital condyle. Above this facet the anterior margin of the neural spine is embayed by a deep semicircular cleft. On the medial side of the neural arch is the axial postzygapophysis. The zygapophysial facet is shallowly concave and oval, except where it is flattened against the edge of the bone.

Fragments of two cervical centra are preserved with TMM 42452-1. These are typically hadrosaurian in being opisthocoelous with a thick ventral keel. The cranial ends of the centra are elevated relative to the posterior ends. The neural arches appear to be fused to their respective centra.

At least one cervical rib is nearly completely preserved in the holotype. It shows a capitular head that extends medioventrally from the ventral edge of the shaft. The tubercular head extends medially from the dorsal edge of the shaft, which forms a somewhat thick elongate plate. The latter is divided by a low rounded ridge. The medial face of the shaft is medially convex around an anteroposterior axis between the capitular process and the base of the tubercular facet.

Sacral vertebrae. A single left sacral ‘rib’ is all that is left of the *Aquilarhinus* sacrum. It consists of an expanded base originally rounded in lateral profile, with a dorsal airfoil-shaped facet for articulation with the neural arch. This base tapers gently into the stout shaft that

expands distally forming a plate, most of which is missing. This plate, along with the shaft itself, was orientated posterodorsally, resulting in a twisted shaft.

Appendicular skeleton

Manus. The recovered carpal of TMM 42452-1 (Fig. 11) is similar in shape to the 'large tetrahedral' carpal observed in other hadrosaurids (e.g., Horner 1979; Davies 1983; Prieto-Márquez 2007). Its surface is irregularly pitted, mostly along the edges and at the corners, suggesting that the element may not have completely ossified. The bone is triangular in longitudinal cross-section. One surface of the carpal is dominated by a large, oval facet that appears to be an articular surface. This surface itself is warped in three dimensions; careful testing shows that it fits with some precision over the head of metacarpal II, but this is at odds with the interpreted position of other such tetrahederal carpals (Prieto-Márquez 2007).

The metacarpus is very narrow and digit I is missing as in all other hadrosauirds (Horner *et al*. 2004). Metacarpals II through IV are narrow, curved slightly abaxially, and somewhat trapezoidal in cross-section. They are arrayed in a U-shape in collective cross-section as in other hadrosaurids (Dilkes 1993) and very large-bodied terrestrial tetrapods (Bakker 1986), with their shafts slightly imbricated (long-axis directed anteromedially) due to axial twisting. Along with phalanx II-1, the distal ends of metatarsals III and IV form the axis of the hyperextendable joint between the metacarpus and digits.

Proximally, the metacarpal heads converge, all with slightly mediolaterally pinched surfaces except for the relatively broad head of metacarpal III. Passing ventrally, metacarpals II

and V diverge from the central axis of the manus near the wrist. In contrast, metacarpals III and IV diverge much less, and do so farther from the wrist.

The manual phalanges of TMM 42452-1 (Fig. 11) represent only the first two ranks, apart from the third phalanx of digit V. Absence of the distalmost phalanges suggests a distal-proximal disarticulation sequence, and perhaps decomposition in the presence of water. The metacarpal/phalangeal joints of the inner three central digits in this specimen, and indeed of all hadrosaurids (Brett-Surman & Wagner 2007), suggests loss of ginglymous morphology and evolution toward plane joints. The first rank of unguals on digits II-IV are distinctly offset such that they curve anteromedially during extension. These may have been bound by ligaments like the metacarpus, rather than splaying proximally.

The second rank of phalanges on digits II-IV is 'wedge shaped,' axially foreshortened, more so medially, with strongly saddle-shaped proximal and distal articular surfaces (concave and convex, respectively). In digits II and III the lateral condyle is the larger. This morphology also brings the rotational plane more anteromedially. A distinctly expanded ventral lip of the proximal articular surface of the second rank of phalanges forms a small flexor tubercle.

The result of the slight plantar displacement of the joint axes is that the manus supinates, pivoting slightly on the ground as the forelimb retracts. As in *Gryposaurus* '*incurvianus*' (= *G. notabilis*, Parks 1920; Prieto-Marquez 2010c), the wrist rotated during forward progression, as might be expected for a quadrupedal animal that holds its elbows slightly offset from the sagittal plane to clear its gut (e.g. Fujiwara & Hutchinson 2012; contra Bakker 1986; Paul & Christiansen 2000).

Phalanx IV-2 is block-like, but the inner (medial) condyle of phalanx IV-2 is more rounded than the smaller, more linear lateral condyle. This suggests that the distal portion of

digit IV was slightly divergent posterolaterally, a situation evident in other hadrosaurids (Parks 1920; 1922; Rozhdestvensky 1957; Prieto-Márquez 2007).

Digit V is similar to that of other iguanodontians (Norman 2004), shorter than the other digits, divergent, and probably prehensile. The fit of the bones suggests that metatarsal V may have been closely applied to metatarsal IV, but it also may have been mobile at the wrist. Three phalanges are preserved, but the third has a smooth distal articular surface suggesting that a fourth was present.

Ilium. This pelvic element is represented by a right postacetabular process (TMM 42452-1, Fig. 12A, B). The process is a thick suboval bony plate (TMM 42452-1, Fig. 12A, B). The process gently tapers posteroventrally. The dorsal margin is straight and heavily eroded, with fragments missing anteriorly. The posterior extent of the ventral margin is slightly offset laterally from the dorsal border, producing a gentle twist about the longitudinal axis of the bone. The medial face of the postacetabular process shows no attachments for sacral ribs, as is common in hadrosaurids (Dilkes 1983). There is a prominent ridge which begins at the posterodorsal margin of the distal end of the process and is obliquely directed anteroventrally. This ridge forms the dorsal border of a roughly textured facet orientated medially and slightly ventrally.

Ischium. A fragmentary ischium preserved with the holotype, TMM 42452-1 (Fig. 12C, D), includes part of the iliac process and the proximal segment of the shaft. The dorsal articular region of the iliac process is eroded away and much of its surface, particularly on the medial side, is heavily abraded. Distally, the ischiadic shaft twists medially along its longitudinal axis.

Astragalus. This element is incompletely represented by both astragali of TMM 42452-1. The right astragalus consists of an abraded fragment of the tibial articular surface. The left element includes most of the main body, missing the anterior and posterior ascending processes and the calcaneal articular surface (Fig. 13A, B). As in all hadrosaurids (Brett-Surman & Wagner 2007), the astragalus is saddle-shaped and mediolaterally expanded. The bone is slightly constricted anteroposteriorly at mid-length of the slightly concave tibial articular surface. Laterally, the astragalus becomes both anteroposteriorly thicker and dorsoventrally deeper, acquiring a convex dorsal surface. This convexity would be bounded anteriorly and posteriorly by the missing ascending processes and receive the concave intermalleolal ventral surface of the tibia.

Pes. Unlike the manus, the pes of *Aquilarhinus palimentus* is poorly known, being solely represented by a phalanx III-1 (Fig. 13C, D) and four unguals (Fig. 13E, F) from the holotype. Phalanx III-1 does not differ from that of other hadrosaurids (Zheng *et al*. 2011). It is subrectangular in dorsal and plantar views, dorsoventrally compressed, and slightly expanded mediolaterally at its proximal and distal ends. The proximal end is substantially deeper than the distal extremity, so that in lateral and medial profile the dorsal surface of the phalanx gently slopes distally.

Likewise, pedal unguals are also typically hadrosaurid in morphology (Zheng *et al*. 2011) in being spade-shaped hoof-like elements as seen in plantar and dorsal (Fig. 13F) views. In lateral and medial views, the ungual phalanx is wedge-shaped. The proximal articular surface is ellipsoidal and mediolaterally expanded.

Hadrosauridae incerta sedis material from Rattlesnake Mountain

Additional hadrosaurid elements were recovered at Rattlesnake Mountain from the same stratigraphic interval as the holotype of *Aquilarhinus palimentus*, some bones within a short distance of the collection site of the holotype (TMM 42452-3 and -4). Although this material might pertain to *A. palimentus*, none of these isolated bones exhibit diagnostic features that would allow for certain attribution. For this reason, we describe this material separately and refrain from referring it to *A. palimentus*.

Braincase wall.TMM 45947-489 (Fig. 14M-P) consists of parts of the skull roof (described below) united with the laterosphenoids, presphenoids, and orbitosphenoids. Sutures between bones are obscure, although on the left side the neurocranium appears to have separated from the adjacent skull roof elements near the sutures. The anterior end of the specimen is broken through the large circular foramen for the olfactory nerves, part of which is formed by a raised ridge on the ventral surface of the frontals (see below), and which separates the olfactory region from the large, spherical cerebral cavity.

Although the sutures cannot be discerned clearly, the buttress ventral to the postorbital articulation can be identified, as can the abraded postorbital articular surface. These structures typically mark the anterior extent of the laterosphenoid and the anterior border of the temporal cavity. Anterior to this is the orbital cavity, the medial wall of which (i.e., the lateral surface of the braincase) is formed by the presphenoid and orbitosphenoid (TMM 45947-489, Fig. 14M-P). The sutural relationships between these two elements are again inscrutable, but by comparison to other hadrosaurid braincases

(e.g., AMNH 5350, Prieto-Márquez, 2010c) it is likely that the preserved portion is mostly orbitosphenoid. There is every possibility that one or more small processes of the laterosphenoid could extend anterior to the buttress, but no evidence. The anteroventral portion of the braincase wall is not preserved.

Two neurovascular features are evident on the lateral braincase surface. The opening for the oculomotor (III) nerve lies just ventral to the level of the postorbital articulation on the lateral surface of the of the braincase, and just anterior to the postorbital buttress. The foramen is round and exits anterodorsolaterally from the braincase. The posterodorsal margin of the foramen for the trochlear (IV) nerve is preserved along the damaged anteroventral margin of the braincase ventral and anterior to the foramen for nerve III. The floor of the endocranial cavity is broken away, and no other openings for cranial nerves are preserved.

Parietal. This element is poorly preserved, with the preserved portion forming the incomplete and abraded posterior region of partial braincase TMM 45947-48 (Fig. 14M-P). It articulates anteriorly with the frontals, but the sutures with those elements are not discernible. An extensive anterolateral process curves laterally forming the anteromedial margin and a small portion of the laterodorsal wall of the supratemporal fossa. Posteriorly, the process merges with its counterpart and the parietal becomes abruptly constricted mediolaterally to form the sagittal crest. The lcrest displays a flattened dorsal surface but does not appear to ascend significantly dorsal to the skull roof in its anterior portion. The posterior extent of the preserved portion of the parietal is heavily abraded, making it impossible to determine if the posterior sagittal crest was elevated as observed in lambeosaurines. The surfaces of the supratemporal fossae extend

posteroventrolaterally from the anterolateral processes and lateroventrally from the sagittal crest. The margins of the supratemporal fenestrae are not preserved.

Frontal. In TMM 45947-48 (Fig. 14M–P), the frontal is missing the anterior and lateral margins. The midline frontal suture is barely discernible, but the anterior portion appears to be angled to the right of the sagittal plane. As shown in TMM 45947-490.1 (Fig. 14G–L), the dorsal surface is flat as far anteriorly as the roof over the olfactory tract, indicating that the frontal likely did not contribute to a nasal arch, if present. As noted above, on the ventral (internal surface) the anterior end of the cerebral fossa is separated from the olfactory recess by an arcuate rounded ridge that rises laterally to form distinct sutural contacts for the presphenoid and orbitosphenoid. Although the anterior end is broken in both available frontals, raised lineations on the surface of the bones suggest that the break occurred near its contact with the prefrontal and nasal, and if so the frontal was embayed anteriorly along that contact.

Postorbital. TMM 45947-490.2 is a central body of a right postorbital (Fig. 14C–F). It preserves the sutural surface for the frontal and parietal along its medial margin, and the rim of the orbit on its lateral edge. The bone is, however, missing its anterior end, as well as the processes for articulation with the jugal and squamosal. The rim of the orbit is swollen dorsoventrally and covered with fine reticulate corrugations. On the ventral surface, a deep socket for articulation with the lateral buttress of the laterosphenoid lies immediately anterior to the anterior border of the supratemporal fenestra.

Scapula. TMM 45947-492 is the proximal end of a left scapula (Fig. 15A, B). The coracoid and glenoid articular facets are mediolaterally compressed and their lateral margins meet at an angle of 150 degrees. The acromion process is horizontal, as is typical of saurolophine hadrosaurids (Brett-Surman and Wagner 2007) and is distally continuous with a relatively narrow deltoid ridge having a poorly defined ventral margin. The preserved portion of the proximal constriction is relatively narrow, being 60% of the distance between the apex of the glenoid and the dorsal margin of the acromion process.

Humerus. TMM 42452-3 is right humerus represented by several fragments (Fig. 15C). The element appears to be relatively slender, with a poorly expanded deltopectoral crest; the maximum anteroposterior breadth of the deltopectoral crest is 1.66 times the minimum diameter of the shaft. This ratio places the expansion of the deltopectoral crest at the lower end of the spectrum of ratios in hadrosaurids (Prieto-Márquez 2010a). The minimum diameter of shaft was calculated from the section of the fragmented distal third of the humerus, corresponding to the distal extent and probably minimum diameter of the humeral shaft (Fig. 15C). The deltopectoral crest accounts for 49% of the length of the humerus and in this ratio, the element falls within the range of non-lambeosaurine hadrosaurids (Prieto-Márquez 2010a). The articular head is a robust and prominent structure forming the proximolateral corner of the humerus (Fig. 15D). The distal end is slightly less expanded than the proximal end and displays an ulnar condyle that is substantially larger than the radial one.

Pubis. TMM 45947-493 is the proximal region of left pubis (Fig. 16A). The iliac process is tetrahedral in overall shape and relatively short, with eroded lateral and dorsal surfaces. Its

posterior surface is smooth and continuous with the acetabular margin. Ventral to the iliac process and the acetabular margin, there is a robust and long rod-like postpubic process that projects posteroventrally. The distal segment of this process is missing. A short eroded ischiadic process extends parallel to and laterally offset from the proximal region of the postpubic process. The prepubic process is nearly entirely missing, with only the proximal-most extent of its proximal constriction remaining.

Ilium. TMM 42309-13 is a left central iliac plate (Fig. 15A, C). The central plate is fairly complete, preserving part of the pubic- and the entire ischiadic process, along with most of the supraacetabular crest. At the anterior corner of the iliac plate, the pubic process is missing its anteroventral apex, but it appears to have been triangular as in all hadrosaurids. Posterior to this process, the acetabular margin is wide and shallow, with a the posterodorsal margin much longer than the anterodorsal. The ischiadic process displays a blunt ventral surface; above this surface, there is a prominent oblique ridge of a relatively large example of the ischiadic tuberosity typical of hadrosaurs (Brett-Surman and Wagner, 2007).

The lateral margin of the supraacetabular crest is abraded but otherwise complete and extends along nearly the entire length of the iliac plate as preserved. In the complete ilium, the breadth of the supraacetabular crest would account for at least 75 to 80% of the length of the iliac plate. Comparatively wide supraacetabular crests are found in kritosaurin saurolophines (Prieto-Márquez 2014) and among non-hadrosaurid hadrosauroids like *Tanius sinensis* (Wiman 1929), *Lophorothon atopus* (Langston 1960), or *Tethyshadros insularis* (Dalla Vecchia 2009). In lateral view, the crest is V-shaped and asymmetrical, with a profile that is strongly skewed posteriorly. The apex of the supraacetabular crest extends ventrally to a level slightly less than half the depth

of the iliac plate. In this regard, the crest of *Aquilarhinus palimentus* is less expanded than that of most hadrosaurids (Prieto-Márquez 2010a). As is typical of saurolophid hadrosaurids (Prieto-Márquez 2011), this apex lies anterodorsally relative to the posteroventral corner of the lateral ridge of the ischiadic tuberosity.

Femur. Fragments of a left femur are preserved (TMM 45947-491, Fig. 16A-D) but most of the shaft is missing. The head is hemispherical and separated from the greater trochanter by a marked proximal constriction. Anterior and posterior surfaces of the greater trochanter are broken, but the base of the lesser trochanter indicates that is was offset laterally. The distal articulation exhibits a prominent anterior intercondylar groove separating the lateral and medial condyles. The lateral condyle is particularly narrow mediolaterally, with a well-developed fossa on its lateral surface. Overall, the femur is indistinguishable from those of other hadrosaurids.

Tibia. Fragments of two left tibiae were collected (TMM 42452-4, Fig. 16E, F). The distal end is only moderately expanded. The astragalar articular surface is not markedly inset compared to the calcaneal surface, and as a result the external and internal malleoli extend to nearly the same level distally. As with the femur, the tibiae are not significantly different from those of other hadrosaurids.

Phylogenetic relationships of *Aquilarhinus palimentus*

The phylogenetic position of the new species was inferred using parsimony. In addition to *Aquilarhinus*, the taxonomic sample included 63 hadrosauroid taxa (14 outgroup species outside

of Hadrosauridae, three non-saurolophid hadrosaurids, 24 saurolophines, and 22 lambeosaurines). The data set consisted of 279 equally weighted morphological characters (195 cranial and 84 postcranial; see Supplemental online material 1 and 2). Multistate characters containing states that are not mutually exclusive and follow a natural morphocline were ordered. This criterion allows for 'crediting' shared intermediate states. The optimal tree(s) search was conducted in TNT version 1.1 (Goloboff *et al*. 2008). A heuristic search of 10,000 replicates using random addition sequences was performed, followed by branch swapping by tree-bisection-reconnection holding ten trees per replicate. Bremer support (Bremer 1988) was assessed by computing decay indices (Donoghue *et al*. 1992) using TNT. Bootstrap proportions (Felsenstein 1985) were also calculated using TNT, setting the analysis for 5,000 replicates using heuristic searches, in which each search was conducted using 25 random addition sequences with branch-swapping by subtree pruning and regrafting. Ancestral states of crest-related characters (absence/presence of crest, character 179; crest shape, character 182; see Supplemental online material 1) were reconstructed using parsimony and maximum likelihood in Mesquite version 3.51 (Maddison & Maddison 2018).

The analysis resulted in 12 most parsimonious trees (MPTs) of 1,056 steps each (C.I. = 0.43, R.I. = 0.78); the best score was found in 3,687 of the 10,000 replicates. In all trees *Aquilarhinus palimentus* appeared at the base of Hadrosauridae, forming a clade with *Latirhinus uistslani* that is sister to Saurolophidae (Fig. 16). The *Aquilarhinus-Latirhinus* clade is unambiguously supported by the possession of an extremely broad and subcircular posterior margin of the external bony naris.

No unambiguous hadrosaurid synapomorphies are observed in the type of *Aquilarhinus palimentus*. However, the clade consisting of the *Aquilarhinus-Latirhinus* lineage, saurolophids,

their most recent common ancestor and all of their descendants is supported by the following unambiguous synapomorphies: angle of deflection of the anterior ventral margin of the dentary between 17 and 25 degrees; maxilla with complete union of the ectopterygoid ridge and the ventral margin of the facet for the jugal; large anterior maxillary foramen opening on the anterolateral body of the maxilla; and elevation of the dorsal profile of the skull to form a cranial crest. The *Aquilarhinus-Latirhinus* clade demonstrably lacks the following unambiguous saurolophid synapomorphies: more than one functional maxillary tooth per position; dentary tooth crowns with a height/width ratio between 2.8 and 3.3; absence of jugal process, having been reduced to a tubercle; ventral spur of the anterior process of the jugal being as deep as or slightly deeper as it is wide proximally; and subvertically orientated palatine facet of the anterior process of the jugal.

The incerta sedis material is mostly indeterminate. The ilium is clearly hadrosaurid, as shown by many characters: lateral profile of the dorsal margin of the ilium distinctly depressed over the supraacetabular process and dorsally bowed over the proximal region of the preacetabular process; the lateral margin of the iliac peduncle progressively disappears ventrally into the lateral surface of the region adjacent to the acetabular margin; and deep iliac central plate that is at least 80% as tall as it is anteroposteriorly wide. The coracoid is demonstrably not saurolophid due to its concave anteromedial margin.

Discussion

Comparison with pre-mid Campanian hadrosaurids. The fossil record of pre-Campanian and early Campanian hadrosaurids is scarce compared to that of the late Campanian and Maastrichtian (Horner *et al*. 2004; Godefroit *et al*. 2012; 2013). The saurolophine tribe Brachylophosaurini include some of the oldest known hadrosaurids (Freedman Fowler & Horner 2015). The oldest species include *Acristavus gagslarsoni* (from the Wahweap Formation of Utah and Two Medicine Formation of Montana, with an estimated age of 81.4–79 Ma; Gates *et al*. 2011) and *Probrachylophosaurus bergei* (from the Judith River Formation of Montana, with an age of 79.8–79.5 Ma; Freedman Fowler & Horner 2015). Brachylophosaurins share with *Aquilarhinus palimentus* the lightly built jugal with elongate apex of the anterior process and a narrow fan-shaped quadratojugal flange. However, the jugal of *A. palimentus* differs from that of brachylophosaurins in possessing a less expanded posteroventral flange, an elongate and oblique articular facet for the palatine, and spur of the anterior process posteriorly offset relative to the apex of the lacrimal margin. As in all other saurolophids, the brachylophosaurin maxilla lacks a produced jugal process and displays a low, rounded jugal tubercle instead, although it shares with *A. palimentus* a posteriorly inclined ectopterygoid shelf (Prieto-Márquez 2005, fig. 4C; Freedman Fowler & Horner 2015, fig. 5).

Lucas *et al*. (2006) described a partial juvenile saurolophine skeleton from the Mancos Shale of northwestern Colorado, from within the *Baculites maclearni* zone dated to 80.35 Ma. Gates *et al*. (2011) subsequently referred it to Brachylophosaurini based on the morphology of its jugal. Certainly, the jugal of the Mancos Shale hadrosaur is lightly built and displays a sharp apex of the anterior process as in both *Aquilarhinus palimentus* and brachylophosaurins. Regardless, photographs of the specimen (Lucas *et al*. 2006, fig. 2A) show up to two functional teeth in the maxillary dental battery, which is sufficient to distinguish this small specimen

(approximately two thirds of the size of TMM 42452-1) from *A. palimentus*. Maxillae with two functional teeth in the occlusal plane are widespread, not only in brachylophosaurins, but among hadrosaurids in general.

Outside North America, several hadrosaurids have been recorded from lower Campanian-Santonian strata of central and eastern Asia. These include *Aralosaurus tuberiferus* (upper Santonian-lower Campanian strata of the Bostobynskaya Formation of southwestern Kazakhstan; Kordikova *et al*. 2001; Averianov 2007), *Jaxartosaurus aralensis* (Santonian Syuksyuk Formation, Kazakhstan; Averianov & Nessov 1995), and *Tsintaosaurus spinorhinus* (lower Campanian strata of the Jingangkou Formation in eastern China; Young 1958; Prieto-Márquez & Wagner 2013). However, these are lambeosaurines, and are all morphologically quite distinct from *Aquilarhinus palimentus* in showing (to a greater or lesser extent) evidence of dorsal migration of the facial skeleton concomitant with the existence of hollow supracranial ornamentation (Godefroit *et al*. 2004; Wagner, 2004; Prieto-Márquez & Wagner 2013; Wagner & Prieto-Márquez in prep.).

There are a small number of known species of non-saurolophid hadrosaurids. *Eotrachodon orientalis*, from uppermost Santonian strata of the Mooreville Chalk in Alabama, is not only one of the oldest known hadrosaurids but also one of a handful of non-saurolophid species (Prieto-Márquez *et al*. 2016b). *E. orientalis* differs from *A. palimentus* in possessing a maxilla with shorter ectopterygoid shelf (less than 35% of the maxillary length) and incomplete union of the ventral spur of the jugal facet and the ectopterygoid ridge (Prieto-Márquez *et al*. 2016a, fig. 6). In addition, the anterior apex and premaxillary shelf of the maxilla of *E. orientalis* is angled much more steeply (45 degrees relative to the tooth row) than in *A. palimentus* (30-degree angle), with a proportionately deeper anterior half and shallow posterior third of the

maxilla. The base of the dorsal process of *E. orientalis* lies posterior to the mid-length of the maxilla, whereas in *A. palimentus* it is centred around the mid-length of the bone. In the context of Hadrosauridae, however, both taxa are remarkable in showing a jugal process of the maxilla. The jugal of *E. orientalis* is similarly lightly built, but the anterior process is substantially shorter and relatively deeper (Prieto-Márquez *et al*. 2016a, fig. 10) than in *A. palimentus*. The nasal of *E. orientalis* is not reflected into a crest. Most significantly, unlike *A. palimentus* the symphysial process of the dentary of *E. orientalis* is medially shorter and lacks the dorsal curvature present in the former ((Prieto-Márquez *et al*. 2016a, fig. 18).

Hadrosaurus foulkii from Campanian strata of the Woodbury Formation in Haddonfield, New Jersey (Leidy 1858; Prieto-Márquez *et al*. 2006) is younger than *Aquilarhinus palimentus*, but is likewise a non-saurolophid hadrosaurid. All that is known of the skull of *H. foulkii* are various teeth and a handful of maxillary fragments (Prieto-Márquez et al. 2006), and only the dentition shows informative overlapping characters with *A. palimentus*. The height/width proportion of dentary tooth crowns is similar in both hadrosaurids, 2.65 in *H. foulkii* (Prieto-Márquez *et al*. 2006) and 2.4 in *A. palimentus*. Also in both species, both maxillary and dentary teeth show a single median carina (Prieto-Márquez *et al*. 2006). Despite the paucity of directly-comparable morphology, phylogenetic analysis demonstrates that the two species are distinct (i.e., they are not sister species).

A fragmentary specimen from the upper Campanian Cerro del Pueblo Formation in northern Mexico formed the basis of the holotype of the non-saurolophid hadrosaurid *Latirhinus uitstlani* (Prieto-Márquez & Serrano Brañas 2012). Unfortunately, the only comparable cranial element between the two hypodigms is the nasal. Both nasals of both species exhibit an extremely broad, arcuate posterior margin of the osseous narial foramen that separates both

species from the rest of hadrosaurids. Indeed, the curvatures are a surprisingly close match (Fig. 17). However, the nasal of *L. uitstlani* differs from that of *A. palimentus* in displaying a significantly dorsoventrally deeper supranarial process (Fig. 17A-C). The greater depth of the supranarial process of *L. uitstlani* becomes even more significant when taking into account that the entire dorsal margin including the internarial articular facet is missing (Fig. 17A). In contrast, the corresponding segment of the shallower supranarial process of *A. palimentus* is entirely preserved (Fig. 17B). There is no evidence that the supranarial process becomes thicker with size in other hadrosaurids, so we doubt that this difference is due to ontogeny.

Comparison with *Gryposaurus* and other saurolophines with arched nasals. The presence of a gentle arch on the dorsal surface of the nasals of *Aquilarhinus palimentus* is reminiscent of the nasal crest in species of the saurolophine *Gryposaurus*. *Gryposaurus* ranges from the early Campanian (Horner 1992; Prieto-Márquez 2012) to possibly the late Maastrichtian (Lehman *et al*. 2016) and are distributed from southern Canada to southwestern Texas (Bertozzo *et al*. 2017). Notably, *G. latidens*, from lower Campanian strata of the Two Medicine Formation of Montana (Horner 1992), represents one of the oldest known hadrosaurids with an estimated age of 80 Ma (Horner *et al*. 2001). A nasal arch is also present in *Rhinorex condrupus*, a sister taxon to *Gryposaurus* spp. from the Neslen Formation of eastern Utah, in late Campanian strata dated to 75–74.5 Ma (Gates & Sheetz 2014). Despite sharing an arcuate dorsal profile of the nasal, *A. palimentus* is clearly different from *R. condrupus* and *Gryposaurus* spp. The external bony naris (at least the dorsal extent) of *Gryposaurus* spp. and *R. condrupus* is significantly narrower anteroposteriorly (e.g., Prieto-Márquez 2010c, fig. 5; Gates & Scheetz 2014, fig. 3) than that of *A. palimentus* (Fig. 4). The maxilla of *Gryposaurus* shows a jugal tubercle instead of a jugal

process (e.g., *G. latidens* MOR 478-5-24-8-7) and its premaxillary shelf is steeply inclined at least 40 degrees relative to the tooth row (e.g., *G. notabilis* ROM 873) compared to the less inclined shelf of *A. palimentus* (30 degrees). Finally, the anterior process of the jugal of *Gryposaurus* (e.g., *G. notabilis* CMN 2278) and *R. condrupus* (Gates & Scheetz 2014, fig. 3) is substantially deeper with a relatively short anterior apex, compared to the shallow process and long apex of *A. palimentus* (Fig. 9A).

Naashoibitosaurus ostromi is a kritosaurin saurolophine (Prieto-Márquez 2014) originally described by Lucas & Hunt (1993) on the basis of a skull and fragmentary postcranium. The nasals display a low but acute arch. Unlike *Aquilarhinus palimentus*, however, the nasal crest of *N. ostromi* lies farther posterodorsally relative to the posterior margin of the external bony naris. Most notably, the posterodorsal margin of the external bony naris is very narrow in *N. ostromi*, less than half the width of the broad subcircular margin enclosed by the nasal of *A. palimentus*. In addition, a deep circumnarial fossa excavates the lateral surface of the nasal surrounding the external bony naris of *N. ostromi*, whereas the fossa is distinctly shallower in *A. palimentus*. As in other hadrosaurids, but unlike *A. palimentus*, the maxilla of *N. ostromi* shows a dorsal jugal tubercle rather than a jugal process and the occlusal plane displays a maximum of two functional teeth. The dorsal surface of the premaxillary shelf is concave and substantially narrower, about half the width of that in *A. palimentus*. Similarly, the palatal process of *N. ostromi* is much shallower, about half the depth seen in *A. palimentus*.

Trophic specialisations in *Aquilarhinus palimentus*. Although the premaxillae of *A. palimentus* were not recovered, there is no indication that the bizarre mandibular symphysial configuration in this species was related to the circumnarial structure, nor is it likely to be related

to any part of the vocal, thermoregulatory, defensive, or other physiological behavioural systems functionally linked to the rostrum. It is here considered more likely that the autapomorphic dentary symphysis is linked to restructuring of the rostrum for a unique feeding strategy. The projection and curvature of the symphysial processes of the dentary, nearly horizontal palatines, and wide nasals all suggest that this animal was broad snouted, if not simply broad-headed, also suggesting trophic adaptation. The dentaries and their symphysial processes would have met in a W-shaped section anteriorly. Assuming the predentary retained its ancestral relationships to the features of the anterior dentary, it would have been shaped like two trowels laid side to side. The raised symphysis might have led to a raised ridge that passed between the concave predentary fossae along the midline, much like the strengthening ridge leading from the handle onto the blade of a spade or shovel. The anterior extension of the symphysial processes, and the general proportions of the dentaries, suggests that the predentary may have been relatively long.

The hypothesized shovel-shaped 'bill' and widening of the skull in *Aquilarhinus palimentus* may have been adapted to shoveling out and scooping up vegetation. The central reinforcing ridge developed from the dentary symphysis would produce two strong arches in cross-section to resist the strain of pushing through sediment or vegetation. The dentary was straightened relative to ancestral hadrosaurids, likely in order to bring the predentary into alignment with the axis of the mandibles, reducing bending stress along the length of the bone and keeping material from falling out of the predentary. The widening of the mandible, and corresponding widening of the cranium, produced a wider 'scoop.'

The adaptations of this animal, as interpreted here, bring to mind those of gomphotherid proboscideans, sirenians, hippopotami, the South American pyrotheres, and especially desmostylians. These groups are or were relatively large bodied herbivorous mammals, many

either semi- aquatic or closely related to aquatic forms. Moreover, these taxa share narial specialisations, as also occur in hadrosaurids. These analogies suggest that *Aquilarhinus palimentus* may have been a paralic, possibly semiaquatic species specialized for digging in loose wet sediment. This habitus is consistent with the facies interpretation of the strata in which the type specimen was found.

Trophic specialization does not seem exceptionally common among hadrosaurids; some non-hadrosaurids (e.g. *Protohadros byrdi*), and the lambeosaurine *Angulomastacator daviesi* (Wagner & Lehman, 2009) have strongly ventrally deflected rostra, but a direct connection to feeding habits has not been proposed. Bakker (1986) and others have proposed trophic specializations based on the diameter of the premaxillary 'beak.' While this is understandable, we feel that until the morphogenetic relationship between the beak and the circumnarial fossa can be explored in detail (Wagner, 2004; Wagner & Prieto-Márquez in prep.), it is wisest to consider this tentative. The conformation of the dentary symphysis in *Aquilarhinus palimentus* is so far the most likely candidate for a clear trophic specialization among hadrosaurids.

Implications for the evolution of the hadrosaurid crest. Ancestral state reconstructions (Supplemental online materials 3–6) for the presence of an osseous cranial crest (in its most simple form, an elevation of the skull roof above the subhorizontal ancestral cranial profile) indicates that the most recent common ancestor of the clade including Saurolophidae and the *Aquilarhinus-Latirhinus* lineage probably sported a crest (Fig. 19A and 20). The presence of a cranial crest was also likely ancestral for saurolophids as a whole, including both lambeosaurines and saurolophines. Therefore, the 'solid crests' of saurolophines and the 'hollow crests' of lambeosaurines are most likely homologous (Hopson 1975; Wagner 2004; Wagner & Prieto-

Márquez in prep.). It would then be less appropriate to say that the crest has evolved several times among saurolophids, and more reasonable to suggest that it is the conformation of the crest, not the presence or absence of a crest, which has been most labile among hadrosaurids.

Both parsimony (Fig. 19B) and maximum likelihood (Fig. 21) optimization methods support the hypothesis that the arched nasals of *Aquilarhinus palimentus* did not evolve independently from those of derived hadrosaurids such as *Gryposaurus* and other kritosaurins that are deeply nested within Saurolophinae but are in fact homologous. This may indicate (as implied by Hopson 1975) that the arched nasal crest is the ancestral conformation of the crest, and all other hadrosaurid crests are ultimately derived from the arched nasal crest.

The lack of sufficient cranial material in *Hadrosaurus foulkii* (Prieto-Márquez *et al*. 2006) prevents ascertaining whether crests were ancestral for Hadrosauridae (Fig. 19A and 20). The unadorned skull of another non-saurolophid hadrosaurid, *Eotrachodon orientalis* (Prieto-Márquez *et al*. 2016a) suggests tentatively that the earliest hadrosaurids lacked supracranial crests. On the other hand, osseous crests must have been lost at least twice within Saurolophinae (*Acristavus gagslarsoni* and Edmontosaurini) and might have been lost in *E. orientalis* as well. So far there is only evidence that enclosure of the nasal passages to form a 'hollow' crest occurred once, in lambeosaurines. However, this must have happened quite early in their evolution, as previously indicated by Prieto-Márquez & Wagner (2013).

Conclusions

Aquilarhinus palimentus represents a new genus and species of hadrosaurid from the early Campanian of southwestern Texas. This taxon is characterized by several

autapomorphies of the facial skeleton, the most remarkable of which consists of a dentary symphysis that is reflected dorsally as well as anteromedially projected. The latter condition, along with evidence of a relatively broad skull, suggest that this hadrosaurid may have fed by shovelling material, possibly soft water plants.

This new species is one of the oldest hadrosaurids and one of the few non-saurolophid hadrosaurids known to date, forming a clade of 'broad-nosed' forms with *Latirhinus uitstlani* that branched off before the major clades Saurolophinae ('solid-crested' and unadorned taxa) and Lambeosaurinae ('hollow-crested' taxa). This adds to the diversity of pre-saurolophid taxa known to date, previously restricted to *Hadrosaurus foulkii* and *Eotrachodon orientalis*, and suggests the existence of a previously unrealized diversity of hadrosaurid lineages that evolved prior to the main radiation of the clade.

Supracranial crests were possibly present ancestrally in non-saurolophid hadrosaurids, as well as in the common ancestor of Saurolophidae, Saurolophinae and Lambeosaurinae. We find evidence in support of nasal arches as the ancestral crest morphology, from which other derived types of supracranial ornaments evolved within saurolophid hadrosaurids.

Acknoweledgments

For access to specimens in their care we are indebted to Wann Langston, Jr., Lynn Murray, Pamela Owen, Chris Sagebiel, Matt Brown and Tim Rowe at the Texas Memorial Museum. We gratefully acknowledge the fine preparation work of Kyle Davies, who skilfully extracted the maxilla, dentary, and quadratojugal of TMM 42452-1. We owe a special debt of gratitude to the

late Wann A. Langston, Jr., for supervising the collection of TMM 42452-1, and supporting the authors in their research on the Cretaceous Big Bend ecosystem. We are also grateful to Elisabeth Freedman Fowler and Terry A. Gates for providing many insightful comments that greatly improved the quality of the manuscript. Funds for the examination of fossil specimens was provided by a Bass Postdoctoral Fellowship from the Field Museum of Natural History. This study was supported by the Ramón y Cajal Program (RyC-2015-17388), the Ministry of Economy, Industry and Competitivity of Spain (grant CGL2016-73230), and the CERCA Program of the Generalitat de Catalunya to APM, a Texas Tech University Graduate School Summer Thesis Research Grant, a Texas Tech Department of Geosciences John P. Brand Scholarship, and a research grant from Sigma Xi National Scientific Honor Society to JRW. This work is partly a product of MS thesis research conducted by JRW under the supervision of TML in the Department of Geosciences, Texas Tech University.

References

Bakker, R.T. 1986. *The Dinosaur Heresies: New Theories Unlocking the Mystery of Dinosaurs and Their Extinction*. New York, NY: Citadel Press, 481 pp.

Befus, K. S., Hanson, R. E., Lehman, T. M. & **Griffin, W. R.** 2008. Cretaceous basaltic phreatomagmatic volcanism in West Texas: maar complex at Pena Mountain, Big Bend National Park, Texas: *Journal of Volcanology and Geothermal Research*, **173**, 245–264.

Bertozzo, P., Dal Sasso, C., Fabbri, M., Manucci, F. & **Maganuco, S.** 2017. Redescription of a remarkably large *Gryposaurus notabilis* (Dinosauria: Hadrosauridae) from Alberta. Canada. *Memorie della Società Italiana di Scienze Naturalie del Museo Civico di Storia Naturale di Milano*, **43**, 1–56.

Bremer, K. 1988. The limits of amino acid sequence data in angiosperm phylogenetic reconstruction. *Evolution*, **42**, 795–803.

Brett-Surman, M. K. & **Wagner, J. R.** 2007. Discussion of character analysis of the appendicular anatomy in Campanian and Maastrichtian North American hadrosaurids—variation and ontogeny. Pp. 135-169 in K. Carpenter (ed.) *Horns and Beaks. Ceratopsian and Ornithopod Dinosaurs*. Indiana University Press, Bloomington.

Breyer, J. A., Busbey, A. B., Hanson, R. E., Befus, K. E., Griffin, W. R., Hargrove, U. S. & **Bergman, S. C.** 2007, Evidence for Late Cretaceous volcanism in Trans-Pecos, Texas: Journal of Geology 115, p. 243–251.

Brink, A. A. 2016. *An early Campanian (Late Cretaceous) mammalian fauna from the lower shale member of the Aguja Formation in the Big Bend region of Texas*. Ph.D. dissertation, Texas Tech University, 285 pp.

Cifelli, R. L. 1994 Therian mammals of the Terlingua local fauna (Judithian), Aguja Formation, Big Bend of the Rio Grande, Texas. *University of Wyoming Contributions to Geology*, **30**, 117–136.

Cope, E. D. 1870. Synopsis of the extinct Batrachia, Reptilia and Aves of North America. *Transactions of the American Philosophical Society*, **14**, 1–252.

Davies, K. L. 1983. *Hadrosaurian dinosaurs of Big Bend National Park, Brewster County, Texas*. Unpublished M.S. thesis, University of Texas, 235 pp.

Dalla Vecchia, F. M. 2009. *Tethyshadros insularis*, a new hadrosauroid dinosaur (Ornithischia) from the Upper Cretaceous of Italy. *Journal of Vertebrate Paleontology*, **29**, 1100–1116.

Dilkes, D.W. 1993. *Growth and locomotion in the hadrosaurian dinosaur Maiasaura peeblesorum from the Upper Cretaceous of Montana*. Unpublished Ph.D. dissertation, University of Toronto, 425 pp.

Dollo, L. 1888. Iguanodontidae et Camptosauridae. *Comptes Rendus de l'Académie des Sciences*, **106**, 775–777.

Donoghue, M. J., Olmstead, R. G., Smith, J. F. & **Palmer, J. D.** 1992. Phylogenetic relationships of *Dipsacales* base don rbcL sequences. *Annals of the Missouri Botanical Garden*, **79**, 672–685.

Edmund, G. 1957. On the special foramina in the jaws of many ornithischian dinosaurs. *Contributions of the Royal Ontario Museum, Division of Zoology and Palaeontology*, **48**, 1–14.

Erickson, G. M., Krick, B. A., Hamilton, M., Bourne, G. R., Norell, M. A., Lilleodden, E. & **Saywer, W.G.** 2012 Complex dental structure and wear biomechanics in hadrosaurid dinosaurs. *Science*, **338**, 98–101.

Evans, D. C. 2006 Nasal cavity homologies and cranial crest function in lambeosaurine dinosaurs. *Paleobiology*, 32, 109–125.

Evans, D. C., Ridgely, R. & **Witmer, L. M.** 2009 Endocranial anatomy of lambeosaurine hadrosaurids (Dinosauria: Ornithischia): a sensorineural perspective on cranial crest function. *Anatomical Record*, **292**, 1315–1337.

Felsenstein, J. 1985. Confidence limits on phylogenies: an approach using the bootstrap. *Evolution*, **39**, 783–791.

Freedman Fowler, E. & **Horner, J. R.** 2015 A new brachylophosaurin hadrosaur (Dinosauria: Ornithischia) with an intermediate nasal crest from the Campanian Judith River Formation of north central Montana. *PLoS ONE*, **10**, e0141304. Doi: 10.1371/journal.pone.0141304

Fujiwara, S. & Hutchinson, J.R. 2012. Elbow joint adductor movement arm as an indicator of forelimb posture in extinct quadrupedal tetrapods. *Proceedings of the Royal Society,* **279**, 2561-2570.

Gates, T. A. & **Sampson, S. D.** 2007. A new species of *Gryposaurus* (Dinosauria: Hadrosauridae) from the late Campanian Kaiparowits Formation, southern Utah, USA. *Zoological Journal of the Linnean Society*, **151**, 351–376.

Gates, T. A. & **Scheetz, R.** 2015. A new saurolophine hadrosaurid (Dinosauria: Ornithopoda) from the Campanian of Utah, North America. *Journal of Systematic Palaeontology*, **13**, 711–725.

Gates, T. A., Sampson, S. D., Delgado de Jesús, C. R., Zanno, L. E., Eberth, D., Hernández-Rivera, R., Aguillón Martínez, M. C. & Kirkland, J. I. 2007. *Velafrons coahuilensis*, a new lambeosaurine hadrosaurid (Dinosauria: Ornithopoda) from the Late Campanian Cerro del Pueblo Formation, Coahuila, Mexico. *Journal of Vertebrate Paleontology*, **27**, 917–930.

Gates, T. A., Horner, J. R., Hanna, R. R. & **Nelson, C. R.** 2011. New unadorned hadrosaurine hadrosaurid (Dinosauria, Ornithopoda) from the Campanian of North America. *Journal of Vertebrate Paleontology*, **31**, 798–811.

Gates, T. A., Prieto-Márquez, A. & **Zanno, L. E.** 2012 Mountain building triggered Late Cretaceous North American megaherbivore dinosaur radiation. *PLoS ONE*, **7**, e42135. Doi: 10.1371/journal.pone.0042135

Godefroit, P., Bolotsky, Y. L. & **Lauters, P.** 2012. A new saurolophine dinosaur from the latest Cretaceous of Far Eastern Russia. *PLoS ONE*, **7**, e36849. Doi: 10.1371/journal.pone.0036849

Godefroit, P., Bolotsky, Y. L. & **Bolotsky, I. Y.** 2013. Osteology and relationships of *Olorotitan arharensis*, a hollow-crested hadrosaurid dinosaur from the latest Cretaceous of Far Eastern Russia. *Acta Palaeontologica Polonica*, **57**, 527–560.

Goloboff, P. A., Farris, J. S. & **Nixon, K. C.** 2008. TNT, a free program for phylogenetic analysis. *Cladistics*, 24, 774–786.

Gradstein, F. M., Ogg, J. G., Schmitz, M. D. & **Ogg, G. M.** 2012. *The Geologic Time Scale*. Elsevier, Amsterdam, 1144 pp.

Head, J. J. 1998. A new species of basal hadrosaurid (Dinosauria, Ornithischia) from the Cenomanian of Texas. *Journal of Vertebrate Paleontology*, **18**, 718–738.

Heaton, M. J. 1972. The palatal structure of some Canadian Hadrosauridae (Reptilia: Ornithischia). *Canadian Journal of Earth Sciences*, **9**, 185–205.

Hopson, J. A. 1975. The evolution of cranial display structures in hadrosaurian dinosaurs. *Paleobiology*, **1**, 21–43.

Horner, J. R. 1979. Upper Cretaceous dinosaurs from the Bearpaw Shale (Marine) of south-central Montana with a checklist of Upper Cretaceous dinosaur remains from marine sediments in North America. *Journal of Paleontology*, **53**, 566–577.

Horner, J. R. 1983. Cranial osteology and morphology of the type specimen of *Maiasaura peeblesorum* (Ornithischia: Hadrosauridae), with discussion of its phylogenetic position. *Journal of Vertebrate Paleontology*, **3**, 29–38.

Horner, J. R. 1992. Cranial morphology of *Prosaurolophus* (Ornithischia: Hadrosauridae) with descriptions of two new hadrosaurid species and evaluation of hadrosaurid phylogenetic relationships. *Museum of the Rockies Occasional Paper*, **2**, 1–119.

Horner, J. R., Schmitt, J.G., Jackson, F. & **Hanna, R.** 2001. Bones and rocks of the Upper Cretaceous Two Medicine – Judith River clastic wedge complex, Montana. *Museum of the Rockies Occasional Paper*, **3**, 1–14.

Horner, J. R., Weishampel, D. B. & **Forster, C. A.** 2004. Hadrosauridae. Pp. 438–463 in D. B. Weishampel, P. Dodson & H. Osmólska (eds) *The Dinosauria*, *Second Edition*. University of California Press, Berkeley.

Kordikova, E. G., Polly, P. D., Alifanov, V. A., Rocek, Z., Gunnell, G. F. & **Averianov, A. O.** 2001. Small vertebrates form the late Cretaceous and early Tertiary of the northeastern Aral Sea Region, Kazakhstan. *Journal of Paleontology*, **75**, 390–400.

Lambe, L. M. 1920. The hadrosaur Edmontosaurus from the Upper Cretaceous of Alberta. *Memories of the Department of Mines, Geological Survey*, **120**, 1–79.

Langston, W. D. 1960. The vertebrate fauna of the Selma Formation of Alabama. Part 6: the dinosaurs. *Fieldiana, Geology Memoirs*, **3**, 313–363.

Lehman, T. M. 1985. *Stratigraphy, sedimentology, and paleontology of Upper Cretaceous (Campanian – Maastrichtian) sedimentary rocks in Trans-Pecos Texas*. Unpublished Ph.D. dissertation, University of Texas at Austin, 300 pp.

Lehman, T. M. & Busbey, A. B. 2007. *Big Bend field trip guidebook*. Society of Vertebrate Paleontology 67th Annual Meeting, 69 pp.

Lehman T. M., Wick S. L. & **Wagner J. R.** 2016. Hadrosaurian dinosaurs from the Maastrichtian Javelina Formation, Big Bend National Park, Texas. *Journal of Paleontology*, **90**, 333–356.

Lehman, T. M., Wick, S. L., Brink, A. B. and Schiller II, T. A. 2019. Stratigraphy and vertebrate fauna of the lower shale member of the Aguja Formation (lower Campanian) in West Texas. *Cretaceous Research*, **99**, 291–314.

Leidy, J. 1858. *Hadrosaurus foulkii*, a new saurian from the Cretaceous of New Jersey, related to *Iguanodon*. *Proceedings of the Academy of Natural Sciences of Philadelphia* **10**, 213–218.

Lucas, S. L., Spielmann, J. A., Kirkland, J. I., Foster, J. R. & **Sullivan, R. M**. 2006. A juvenile hadrosaurine from the middle Campanian (Late Cretaceous) interval of the Mancos Shale, western Colorado. *New Mexico Museum of Natural History and Science Bulletin*, **35**, 281–291.

Lull, R. S. & Wright, N. E. 1942. Hadrosaurian dinosaurs of North America. *Geological Society of America Special Papers*, **40**, 1–242.

Lund, E. K. & Gates, T. A. 2006. A historical and biogeographical examination of hadrosaurian dinosaurs. *New Mexico Museum of Natural History and Science Bulletin*, **35**, 263–276.

Maddison, W. P. & Maddison, D. R. 2018. Mesquite: a modular system for evolutionary analysis. Version 3.51. http://www.mesquiteproject.org

Marsh, O. C. 1881. Principal characters of American Jurassic dinosaurs. Part IV. *American Journal of Science*, **21**, 417–423.

Norman, D. B. 1980. On the ornithischian dinosaur *Iguanodon bernissartensis* from the Lower Cretaceous of Bernissart (Belgium). *Mémoires de l'Institut Royal des Sciences Naturelles de Belgique*, **178**, 1–103.

Norman, D. B. 2004. Basal Iguanodontia. Pp. 413–437 in D. B. Weishampel, P. Dodson & H. Osmólska (eds) *The Dinosauria*, *Second Edition*. University of California Press, Berkeley.

Ogg, J. G., Hinnov, L. A. & Huang, C. 2012. Cretaceous. Pp. 703–853 in F. M. Gradstein, J. G. Ogg, M. D. Schmitz & G. M. Ogg (eds) *The Geologic Time Scale*. Elsevier, Amsterdam.

Ostrom, J. H. 1961. Cranial morphology of the hadrosaurian dinosaurs of North America. *Bulletin of the American Museum of Natural History*, **122**, 33–186.

Ostrom, J. H. 1962. The cranial crests of hadrosaurian dinosaurs. *Postilla*, **62**, 1–29.

Owen, R. 1842. Report on British Fossil Reptiles. Part 2. *Report of the British Association for the Advancement of Science (Plymouth)*, **11**, 60–204.

Paul, G. S. & Christiansen, P. 2000. Forelimb posture in neoceratopsian dinosaurs: implications for gait and locomotion. *Paleobiology,* **26**, 450-465.

Parks, W. A. 1920. The osteology of the trachodont dinosaur *Kritosaurus incurvimanus*. *University of Toronto Studies, Geological Series*, **11**, 1–74.

Parks WA. 1922. *Parasaurolophus walkeri*, a new genus and species of crested trachodont dinosaur. *University of Toronto Studies, Geological Series*, **13**, 1–32.

Prieto-Márquez, A. 2005. New information on the cranium of *Brachylophosaurus canadensis* (Dinosauria, Hadrosauridae), with a revision of its phylogenetic position. *Journal of Vertebrate Paleontology*, **25**, 144–156.

Prieto-Márquez A. 2007. Postcranial osteology of the hadrosaurid dinosaur *Brachylophosaurus canadensis* from the Late Cretaceous of Montana. Pp. 91–115 in K. Carpenter K (ed) *Horns and beaks: ceratopsian and ornithopod dinosaurs*. Indiana University Press, Bloomington.

Prieto-Márquez, A. 2010a. Global phylogeny of Hadrosauridae (Dinosauria: Ornithopoda) using parsimony and Bayesian methods. *Zoological Journal of the Linnean Society*, **159**, 435–502.

Prieto-Márquez, A. 2010b. Global historical biogeography of hadrosaurid dinosaurs. *Zoological Journal of the Linnean Society*, **159**, 503–525.

Prieto-Márquez, A. 2010c. The braincase and skull roof of *Gryposaurus notabilis* (Dinosauria, Hadrosauridae), with a taxonomic revision of the genus. *Journal of Vertebrate Paleontology*, **30**, 838–854.

Prieto-Márquez, A. 2011. Revised diagnoses of *Hadrosaurus foulkii* Leidy, 1858 (the type genus and species of Hadrosauridae Cope, 1869) and *Claosaurus agilis* Marsh, 1872 (Dinosauria: Ornithopoda) from the Late Cretaceous of North America. *Zootaxa*, **2765**, 61–68.

Prieto-Márquez, A. 2012. The skull and appendicular skeleton of *Gryposaurus latidens*, a saurolophine hadrosaurid (Dinosauria: Ornithopoda) from the early Campanian (Cretaceous) of Montana, USA. *Canadian Journal of Earth Sciences*, **49**, 503–532

Prieto-Márquez, A. 2014 Skeletal morphology of *Kritosaurus navajovius* (Dinosauria: Hadrosauridae) from the Late Cretaceous of the North American south-west, with an evaluation of the phylogenetic systematics and biogeography of Kritosaurini. *Journal of Systematic Palaeontology*, **12**, 133–175.

Prieto-Márquez, A. & **Norell, M. A.** 2010. Anatomy and relationships of *Gilmoreosaurus mongoliensis* (Dinosauria: Hadrosauroidea) from the Late Cretaceous of Central Asia. *American Museum Novitates*, **3694**, 1–49.

Prieto-Márquez, A. & **Serrano Brañas, C. I.** 2012 *Latirhinus uitstlani*, a 'broad-nosed' saurolophine hadrosaurid (Dinosauria, Ornithopoda) from the late Campanian (Cretaceous) of northern Mexico. *Historical Biology*, **24**, 607–619.

Prieto-Márquez, A. & **Wagner, J. R.** 2013. The 'unicorn' dinosaur that wasn't: a new reconstruction of the crest of *Tsintaosaurus* and the early evolution of the lambeosaurine crest and rostrum. *PLoS ONE*, **8**, e82268. Doi: 10.1371/journal.pone.0082268

Prieto-Márquez, A., Weishampel, D. B. & **Horner, J. R.** 2006. The dinosaur *Hadrosaurus foulkii*, from the Campanian of the East Coast of North America, with a reevaluation of the genus. *Acta Palaeontologica Polonica*, **51**, 77–98.

Prieto-Márquez, A., Erickson, G. M. & **Ebersole, J. A.** 2016a. Anatomy and osteohistology of the basal hadrosaurid dinosaur *Eotrachodon* from the uppermost Santonian (Cretaceous) of southern Appalachia. *PeerJ*, **4**, e1872. Doi: 10.7717/peerj.1872

Prieto-Márquez, A., Erickson & **G. M., Ebersole, J. A.** 2016b. A primitive hadrosaurid from southeastern North America and the origin and early evolution of 'duck-billed' dinosaurs. *Journal of Vertebrate Paleontology*, **36**, e1054495. Doi: 10.1080/02724634.2015.1054495

Rozhdestvensky, A. K. 1957. The duck–billed dinosaur *Saurolophus* from the Upper Cretaceous of Mongolia [in Russian]. *Vertebrata PalAsiatica*, **1**, 129–149.

Rowe, T., Cifelli, R. L., Lehman, T. L. & **Weil, A.** 1992. The Campanian Terlingua local fauna, with a summary of other vertebrates from the Aguja Formation, Trans-Pecos Texas. *Journal of Vertebrate Paleontology*, **12**, 472–493.

Sankey, J. T. 2001. Late Campanian southern dinosaurs, Aguja Formation, Big Bed, Texas. *Journal of Paleontology*, **71**, 208–215.

Seeley, H. G. 1887. On the classification of the fossil animals commonly named Dinosauria. *Proceedings of the Royal Society of London*, **43**, 165–171.

Sternberg, C. M. 1936. The systematic position of *Trachodon*. *Journal of Paleontology*, **10**, 652–655.

Waggoner, K. J. 2006. *Sutural form and shell morphology of* Placenticeras *and systematic descriptions of Late Cretaceous ammonites from the Big Bend region, Texas*. Unpublished Ph.D. dissertation, Texas Tech University, 398 pp.

Wagner, J. R. 2001. *The hadrosaurian dinosaurs (Ornithischia: Hadrosauria) of Big Bend National Park, Brewster County, Texas, with implications for Late Cretaceous Paleozoogeography*. Unpublished M.S. thesis, Texas Tech University, 417 pp.

Wagner, J. R. 2004 Hard-tissue homologies and their consequences for interpretation of the cranial crests of lambeosaurine dinosaurs (Dinosauria: Hadrosauria). *Journal of Vertebrate Paleontology*, **24**, 125A–126A.

Wagner, J. R. & **Lehman, T. M.** 2001 A new species of *Kritosaurus* from the Cretaceous of Big Bend National Park, Brewster County, Texas. *Journal of Vertebrate Paleontology*, **21**, 110A–111A.

Wagner, J. R. & **Lehman, T. M.** 2001. An enigmatic new lambeosaurine hadrosaur (Reptilia: Dinosauria) from the Upper Shale Member of the Campanian Aguja Formation of Trans-Pecos Texas. *Journal of Vertebrate Paleontology*, **29**, 605–611A.

Wagner, J. R. & **Lehman, T. M.** 2009. An enigmatic new lambeosaurine hadrosaur (Reptilia: Dinosauria) from the upper shale member of the Campanian Aguja Formation of Trans-Pecos Texas. *Journal of Vertebrate Paleontology*, **29**, 605-611.

Weishampel, D.B., Norman, D.B., Grigorescu, D. 1993. *Telmatosaurus transsylvanicus* from the Late Cretaceous of Romania: the most basal hadrosaurid. *Palaeontology* **36**: 361–385.

Wick, S. L., Lehman, T. M. & **Brink, A. A.** 2015 A theropod tooth assemblage from the lower Aguja Formation (early Campanian) of west Texas, and the roles of small theropod and varanoid lizard mesopredators in a tropical predator guild. *Palaeogeography, Palaeoclimatology, Palaeoecology,* **418**, 229–244.

Wiman, C. 1929. Die Kreide. Dinosaurier aus Shantung. *Palaeontologia Sinica, Series C*, **6**, 1–67.

Young, C. C. 1958. The dinosaur remains of Laiyang, Shantung. *Palaeontologica Sinica, New Series C*, **16**, 53–138.

Zheng, R., Farke, A.A. & **Kim, G.-S.** 2011. A photographic atlas of the pes from a hadrosaurine hadrosaurid. *PalArch's Journal of Vertebrate Palaeontology*, **8**, 1–12.

Supplemental online material

Supplemental online material 1. List of morphological characters used in the phylogenetic analysis.

Supplemental online material 2. Character-taxon matrix used in the phylogenetic analysis.

Supplemental online material 3. Parsimony optimization of the presence/absence of osseous cranial crest in hadrosaurids mapped on each of the 12 most parsimonious trees derived from the phylogenetic analysis.

Supplemental online material 4. Parsimony optimization of osseous cranial crest morphology in hadrosaurids mapped on each of the 12 most parsimonious trees derived from the phylogenetic analysis.

Supplemental online material 5. Results of the maximum likelihood optimization for the absence/presence of osseous cranial crest in hadrosaurids.

Supplemental online material 6. Results of the maximum likelihood optimization of osseous cranial crest shape in hadrosaurids.

Figure captions

Figure 1. Geographic and straigraphic location of the type and referred material of *Aquilarhinus palimentus*. Abbreviations: cl, clay; si, silt; ss, sandstone; cg, conglomerate.

Figure 2. Reconstruction of the skull and mandible of *Aquilarhinus palimentus*. Areas colored in brown indicate bones belonging to the holotype specimen TMM 42452-1.

Figure 3. Left nasal of the holotype specimen (TMM 42452-1) of *Aquilarhinus palimentus*. **A**, lateral view; **B**, interpretive line drawing of the lateral view; **C**, medial view; **D**, interpretive line drawing of the medial view. Dark grey indicates reconstruction, cross-hatching indicates broken surfaces, open circles represent concretionary matrix.

Figure 4. Right nasal of the holotype specimen (TMM 42452-1) of *Aquilarhinus palimentus*. **A**, lateral view; **B**, interpretive line drawing of the lateral view; **C**, medial view; **D**, interpretive line

drawing of the medial view. Dark grey indicates reconstruction, cross-hatching indicates broken surfaces, open circles represent concretionary matrix.

Figure 5. Right maxilla of the holotype specimen (TMM 42452-1) of *Aquilarhinus palimentus*. **A**, lateral view; **B**, interpretative line drawing of the lateral view; **C**, dorsal view; **D**, interpretative line drawing of the dorsal view.

Figure 6. Right maxilla of the holotype specimen (TMM 42452-1) of *Aquilarhinus palimentus*. **A**, medial view; **B**, interpretative line drawing of the medial view; **C**, medioventral view, exposing the occlusal plane of the dental battery; **D**, lateral view showing the area of the tooth row enhanced in E; **E**, detail view of the maxillary dentition in labial view.

Figure 7. Facial elements of the holotype specimen (TMM 42452-1) of *Aquilarhinus palimentus*. **A**, right jugal in lateral view; **B**, interpretative line drawing of A; **C**, right jugal in medial view; **D**, interpretative line drawing of C; **E, F**, lateral and medial views, respectively, of the right quadratojugal; **G**, **F**, interpretative line drawings of E and F, respectively.

Figure 8. Right palatine of the holotype specimen (TMM 42452-1) of *Aquilarhinus palimentus* in **A**, anterior view; **B**, dorsal view; **C**, medial view; and **D**, ventral view; **E**, articulated right palatine, maxilla and jugal in anterodorsolateral view; **F**, articulated right palatine, maxilla and jugal in posterodorsolateral view.

Figure 9. Partial sphenoid of the holotype specimen (TMM 42452-1) of *Aquilarhinus palimentus*. **A**, anterior view; **B**, posterior view; **C**, posteroventral view; **D**, lateral view; **E**, ventral view.

Figure 10. Mandibular elements of the holotype specimen (TMM 42452-1) of *Aquilarhinus palimentus*. **A**, right dentary in lateral view; **B**, right dentary in anterior view; **C**, interpretative line drawing of A, grey indicates reconstrutions; **D, E**, first ceratobranchial in lateral and dorsal views, respectively; **F**, right dentary in medial view; **G**, detail of the dental battery of the right dentary in lingual view; **H,** interpretative line drawing of F; **I**, interpretative line drawing of the right dentary in dorsal view; **J**, right dentary in dorsal view; **K**, fragment of right coronoid process in medial view.

Figure 11. Forelimb elements of the holotype specimen (TMM 42452-1) of *Aquilarhinus palimentus*. Left manus in dorsal, **A**, and palmar, **B**, views, respectively.

Figure 12. Pelvic elements of the holotype specimen (TMM 42452-1) of *Aquilarhinus palimentus*. **A** and **B**, postacetabular process of right ilium in dorsal and lateral views, respectively; **C** and **D**, partial right ischium in lateral and medial views, respectively.

Figure 13. Hindlimb elements of the holotype specimen (TMM 42452-1) of *Aquilarhinus palimentus*. **A** and **B**, left astragalus in dorsal and posterior views, respectively; **C** and **D**, right pedal phalanx III-1 in lateral and ventral views, respectively; **E** and **F**, pedal ungual III in lateral and dorsal, views.

Figure 14. Hadrosaurid facial and neurocranial elements from Rattlesnake Mountain. **A**, **C** and **E,** partial left postorbital (TMM 45947-490.2) in dorsal, lateral and ventral views, respectively. **B**, **D** and **F**, interpretative line drawings of A, C and E, respectively; **G**, **I** and **K**, partial left frontal (TMM 45947-490.1) in medial, ventral and dorsal views, respectively; **H**, **J** and **L**, interpretative line drawings of G, I and K, respectively; **M, O**, partial neurocraneum (TMM 45947-489) in dorsal and right lateral views, respectively; **N, P**, interpretative line drawings of M and O.

Figure 15. Pectoral and forelimb hadrosaurid elements from Rattlesnake Mountain. **A, B**, proximal region of left scapula (TMM 45947-492) in proximal and lateral views, respectively; **C–E**, partial left humerus (TMM 42452-3) in posterior, proximal and distal views, respectively.

Figure 16. Hadrosaurid pelvic and hindlimb elements from Rattlesnake Mountain. **A**, partial left pubis (TMM 45947-493) in lateral view; **B,** central plate of left ilium (TMM 42309-13) in lateral view; **C–F**, left femur (TMM 45947-491) in proximal, posterior, medial and distal views, respectively; **G** and **H**, distal end of right tibia (TMM 42452-4) in posterior and distal views, respectively.

Figure 17. Comparison of the nasals of *Aquilarhinus palimentus* and *Latirhinus uitstlani*. **A**, partial right nasal of *L. uitstlani* (IGM 6583) in medial view; **B**, right nasal of *A. palimentus* (TMM 42452-1) in medial view; **C**, superimposition of the right nasals of *L. uitstlani* and *A. palimentus* in medial view, showing the dorsoventrally broader supranarial process of *L.*

uitstlani; note that while the dorsal margin of the supranarial process is complete and the internarial facet is preserved in *A. palimentus*, it is missing in *L. uitstlani*, implying a substantially wider supranarial process in the Mexican species.

Figure 18. Strict consensus tree showing the phylogenetic position of *Aquilarhinus palimentus* within hadrosaurid dinosaurs.

Figure 19. Parsimony optimization of two characters describing different conditions of the osseous cranial crest in hadrosaurid dinosaurs, mapped on the strict consensus tree resulting from the parsimony phylogenetic analysis. **A**, optimization of the presence/absence of osseous cranial crest; **B**, optimization of the morphology of the osseous cranial crest.

Figure 20. Maximum likelihood optimization of the absence/presence of osseous cranial crest mapped onto one of the 12 most parsimonious trees resulting from the phylogenetic analysis. Taxon font colors indicate the following: red, osseous crest present; blue, osseous crest absent; grey, presence or absence of osseous crest unknown.

Figure 21. Maximum likelihood optimization of osseous cranial crest shape mapped onto one of the 12 most parsimonious trees resulting from the phylogenetic analysis. Colors indicate the following: grey, presence or absence of osseous crest unknown; black, crest absent; dark blue, arcuate protuberance, dorsal to the orbits in adults; light blue, paddle-like posteriorly directed solid crest; green, rod-like posterodorsally directed solid crest; excavated anteriorly facing protuberance, anterodorsal to the orbit; orange, nasal fold rising dorsally or posterodorsally,

laterally excavated, resting over the frontal; red, cockscomb formed by the nasal and a solid plate-like extension of the premaxilla; violet, long and tubular crest, extending posteriorly beyond the occiput and gently arched.

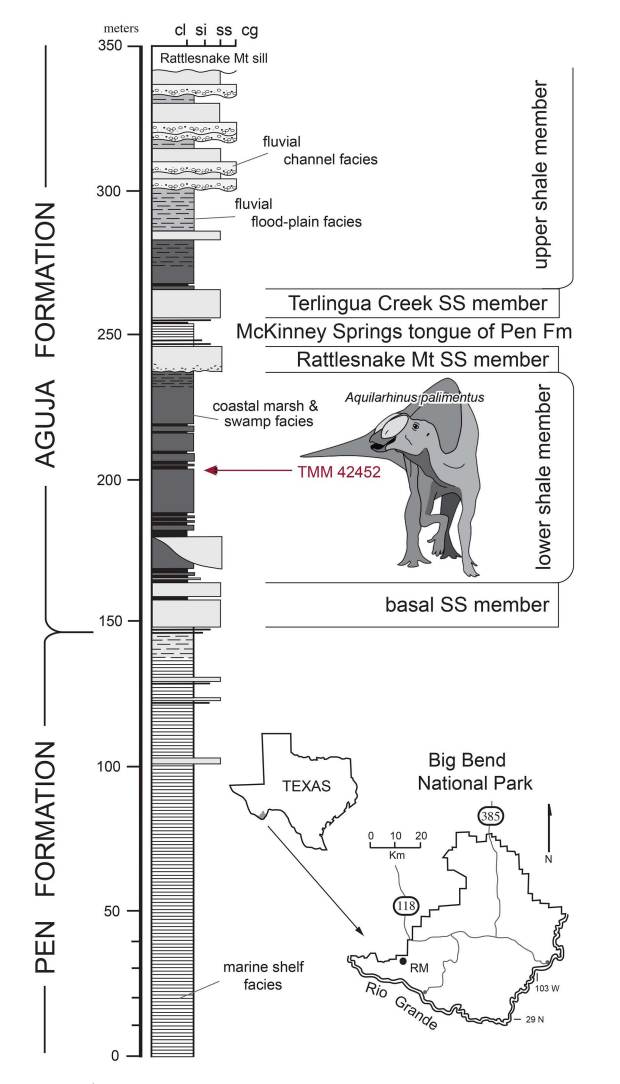
meters
cl si ss cg
350
300
250
200
150
100
50
0
Rattlesnake Mt sill
fluvial
channel facies
fluvial
flood-plain facies
upper shale member
Terlingua Creek SS member
McKinney Springs tongue of Pen Fm
Rattlesnake Mt SS member
lower shale member
Aquilarhinus palimentus
coastal marsh &
swamp facies
TMM 42452
basal SS member
AGUJA FORMATION
PEN FORMATION
marine shelf
facies
TEXAS
Big Bend
National Park
0 10 20
Km
N
385
118
RM
Rio Grande
103 W
29 N

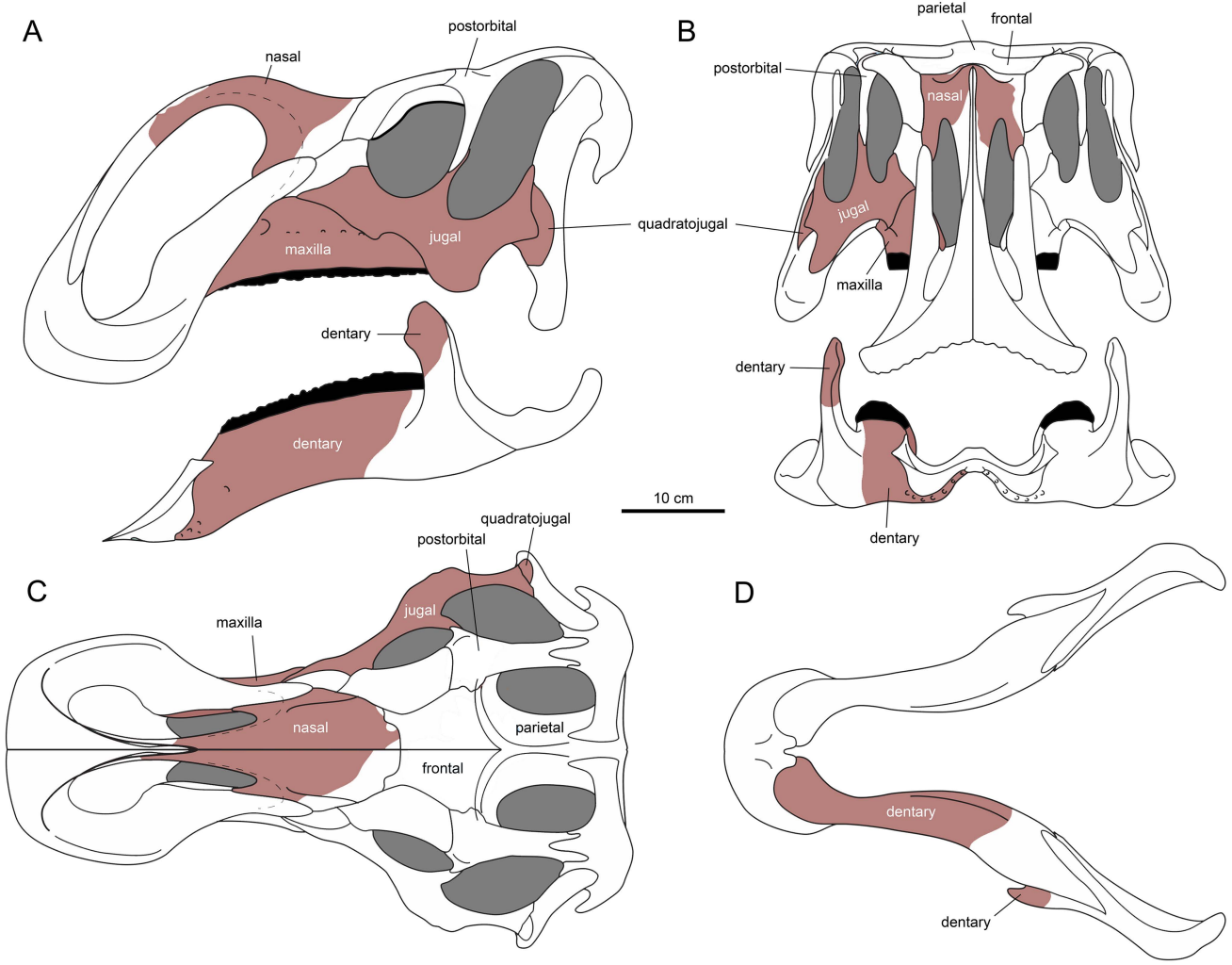
A
nasal
postorbital
maxilla
jugal
quadratojugal
dentary
dentary
B
parietal
frontal
postorbital
nasal
jugal
maxilla
dentary
dentary
10 cm
C
quadratojugal
postorbital
jugal
maxilla
nasal
parietal
frontal
D
dentary
dentary

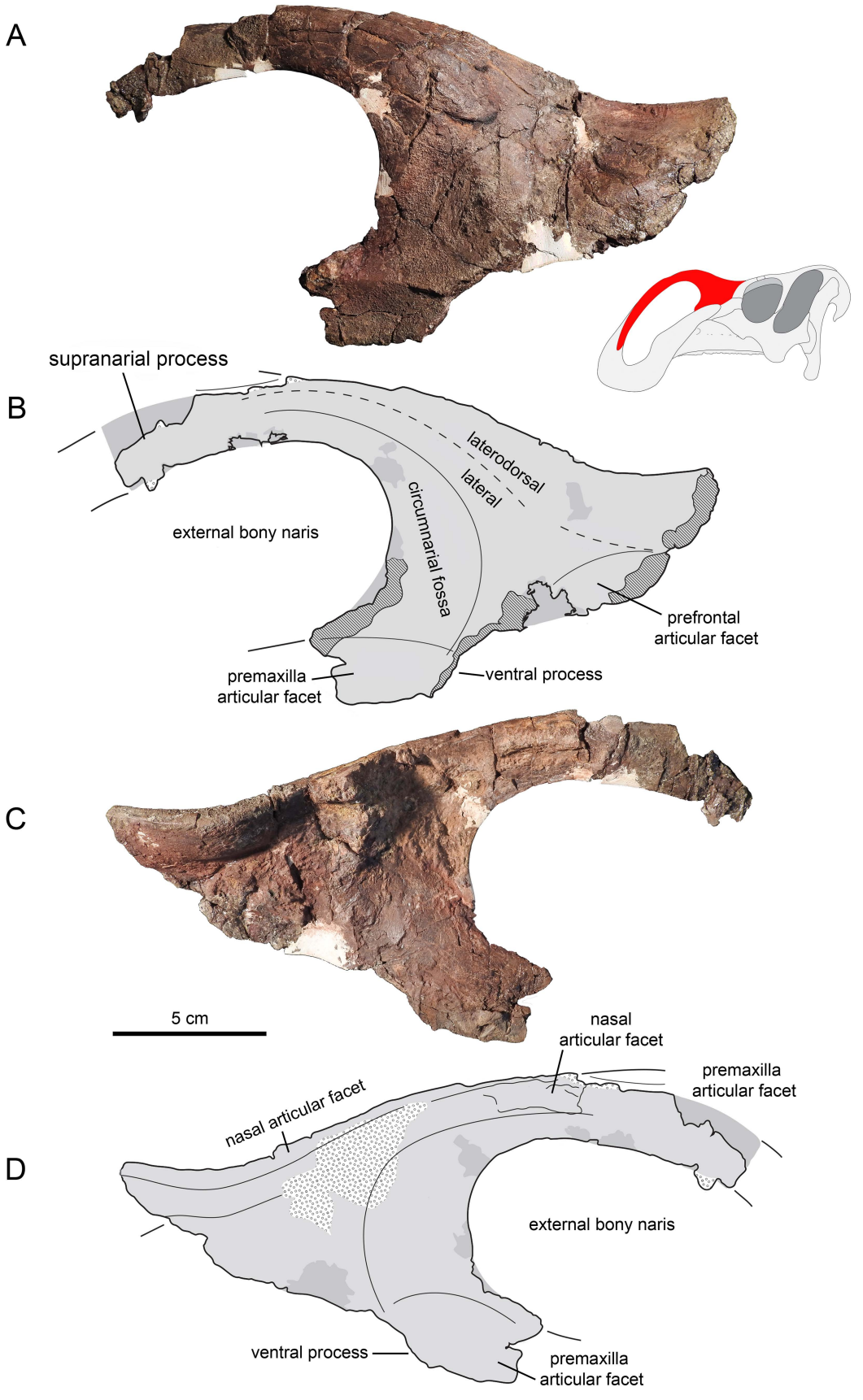
A
B
supranarial process
laterodorsal
lateral
circumnarial fossa
external bony naris
prefrontal
articular facet
premaxilla
articular facet
ventral process
C
5 cm
D
nasal
articular facet
premaxilla
articular facet
nasal articular facet
external bony naris
ventral process
premaxilla
articular facet

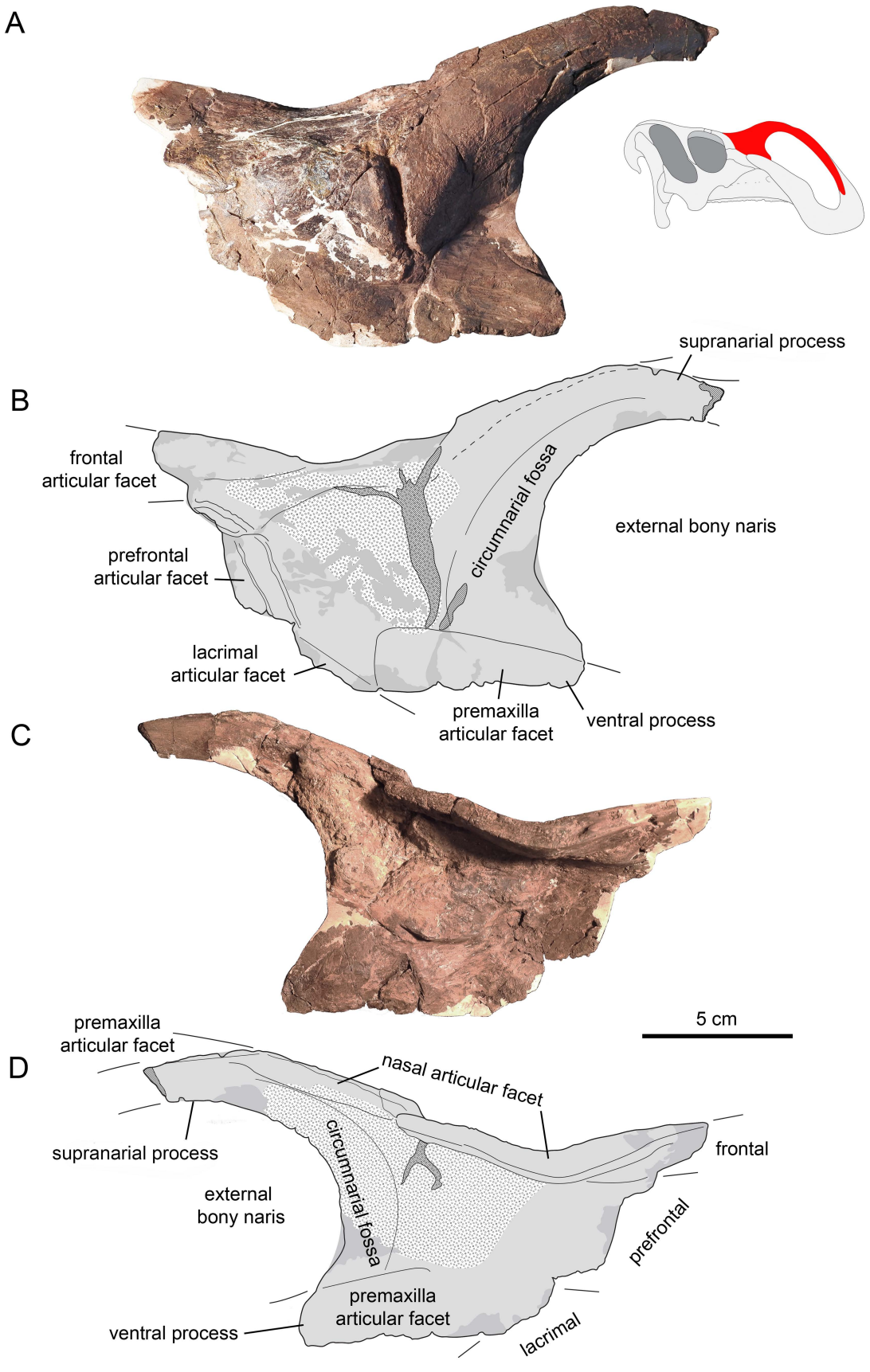
A
B
supranarial process
frontal
articular facet
prefrontal
articular facet
lacrimal
articular facet
circumnarial fossa
external bony naris
premaxilla
articular facet
ventral process
C
5 cm
D
premaxilla
articular facet
nasal articular facet
supranarial process
external
bony naris
circumnarial fossa
frontal
prefrontal
premaxilla
articular facet
ventral process
lacrimal

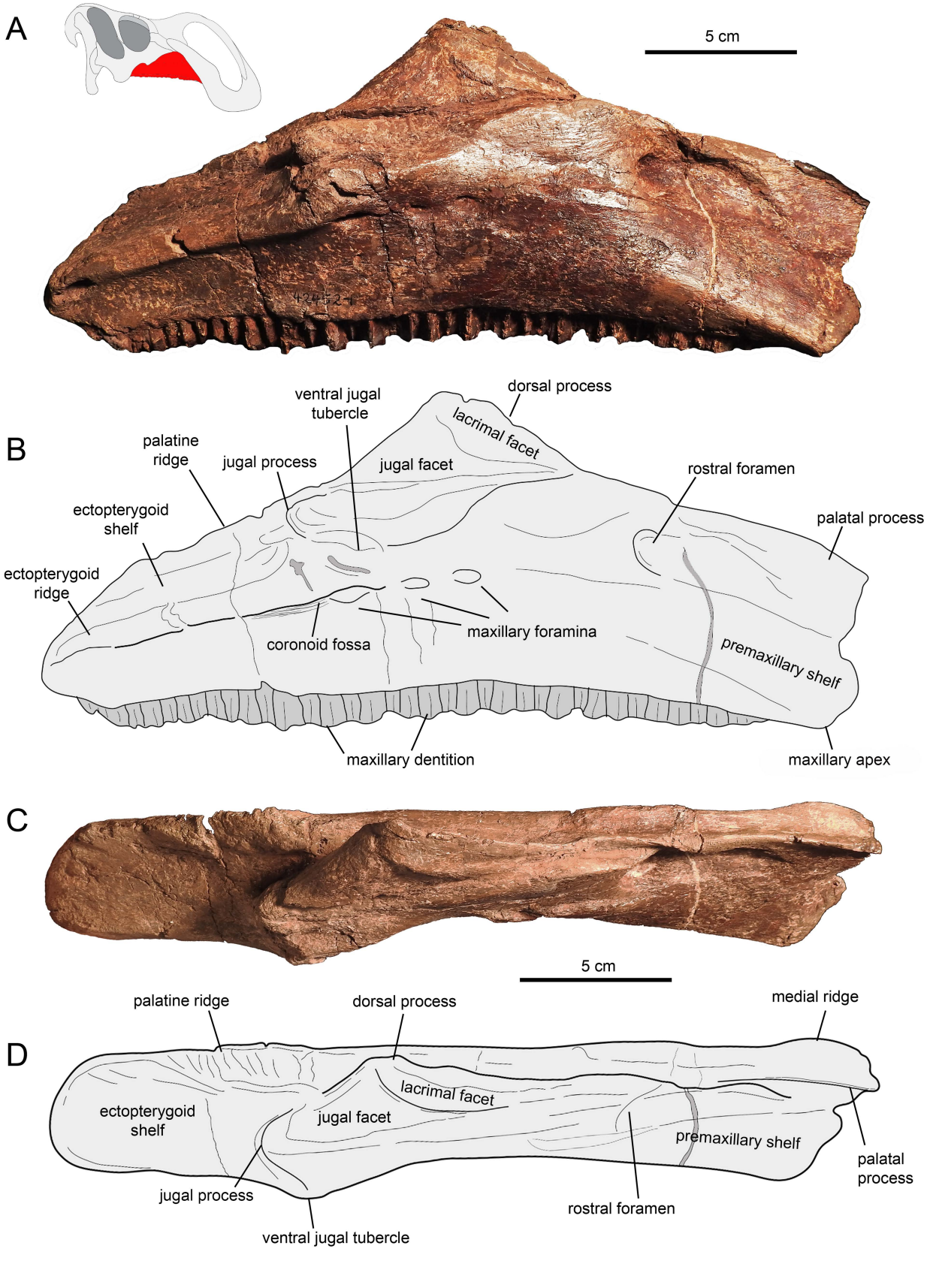
A
5 cm
B
dorsal process
ventral jugal tubercle
lacrimal facet
palatine ridge
jugal process
jugal facet
rostral foramen
ectopterygoid shelf
palatal process
ectopterygoid ridge
maxillary foramina
coronoid fossa
premaxillary shelf
maxillary dentition
maxillary apex
C
5 cm
D
palatine ridge
dorsal process
medial ridge
lacrimal facet
ectopterygoid shelf
jugal facet
premaxillary shelf
palatal process
jugal process
rostral foramen
ventral jugal tubercle

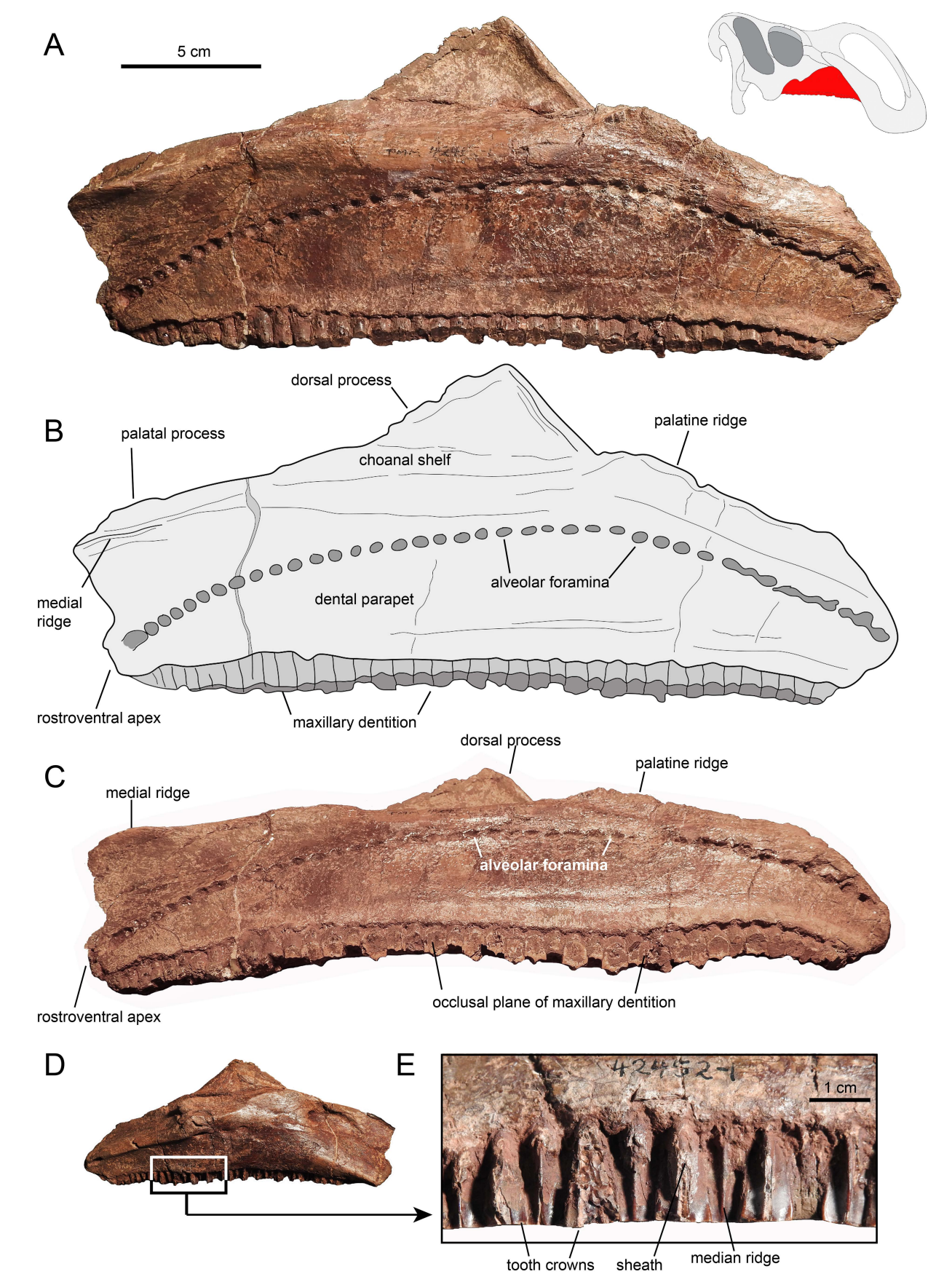
A
5 cm
B
dorsal process
palatal process
choanal shelf
palatine ridge
medial ridge
dental parapet
alveolar foramina
rostroventral apex
maxillary dentition
C
dorsal process
palatine ridge
medial ridge
alveolar foramina
occlusal plane of maxillary dentition
rostroventral apex
D
E
42452-1
1 cm
tooth crowns
sheath
median ridge

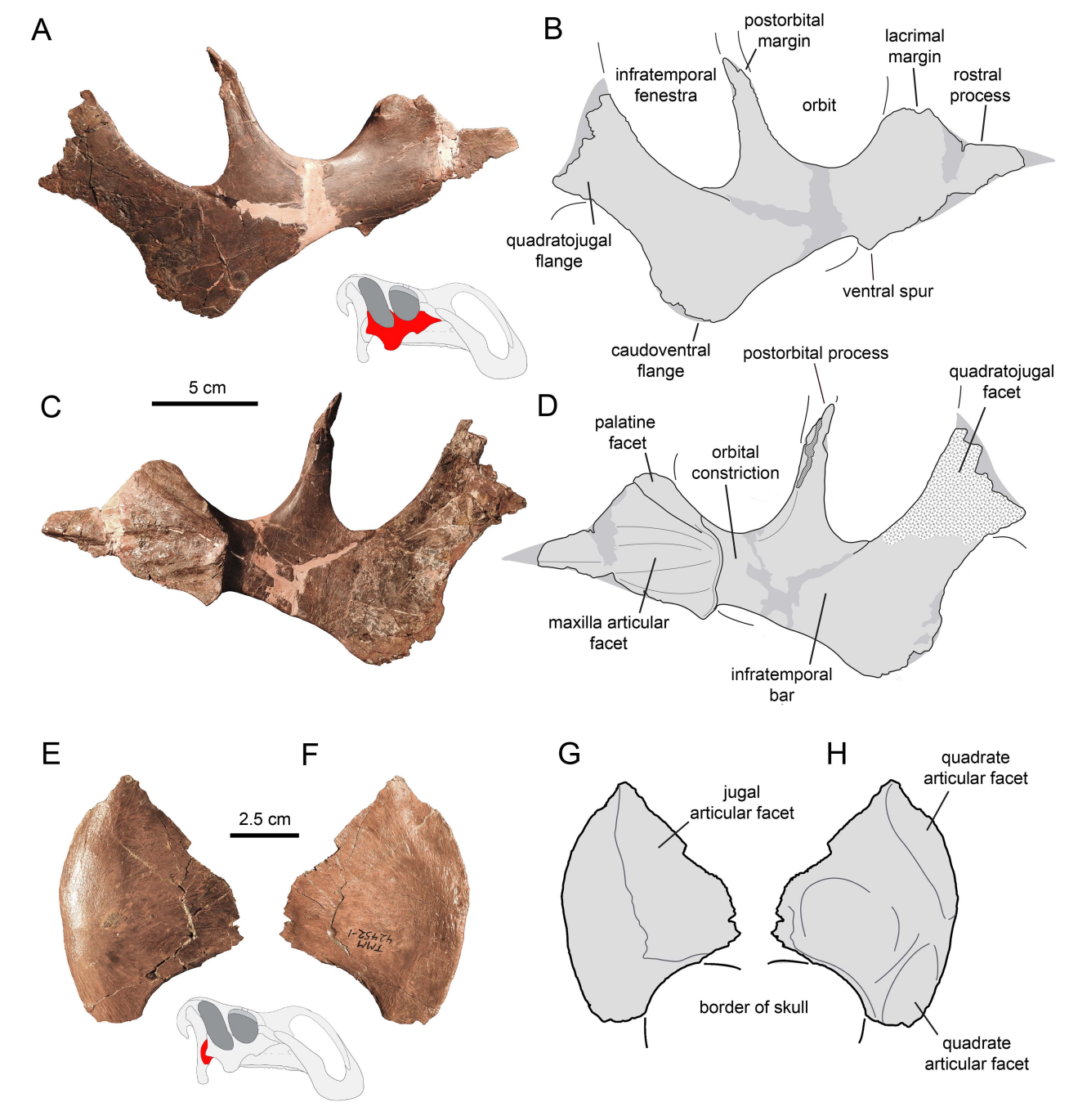
A
B
postorbital margin
lacrimal margin
infratemporal fenestra
orbit
rostral process
quadratojugal flange
ventral spur
caudoventral flange
5 cm
C
D
postorbital process
quadratojugal facet
palatine facet
orbital constriction
maxilla articular facet
infratemporal bar
E
F
2.5 cm
G
H
jugal articular facet
quadrate articular facet
border of skull
quadrate articular facet

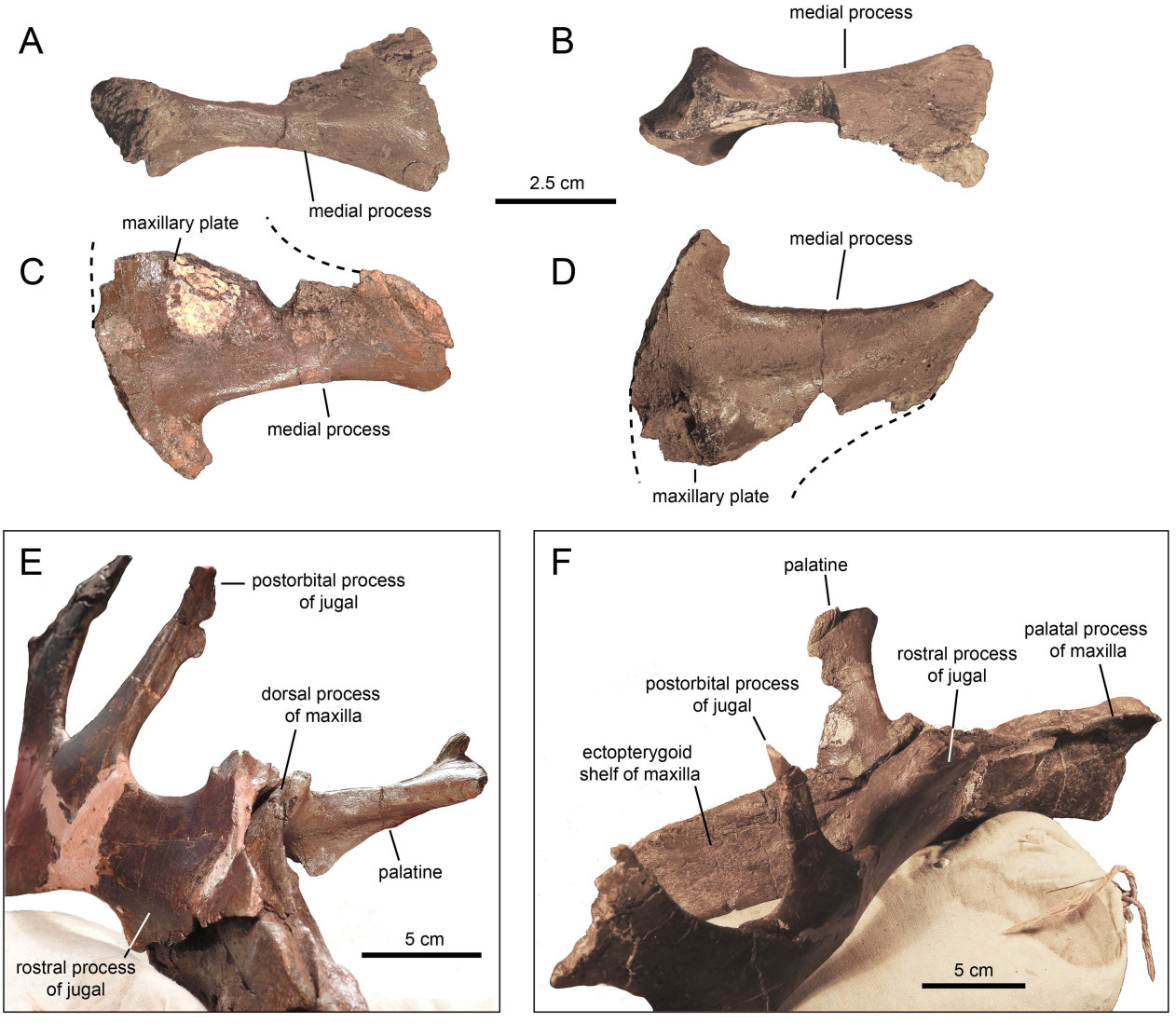
A
medial process
B
medial process
2.5 cm
maxillary plate
C
medial process
D
medial process
maxillary plate
E
postorbital process of jugal
dorsal process of maxilla
palatine
5 cm
rostral process of jugal
F
palatine
palatal process of maxilla
rostral process of jugal
postorbital process of jugal
ectopterygoid shelf of maxilla
5 cm

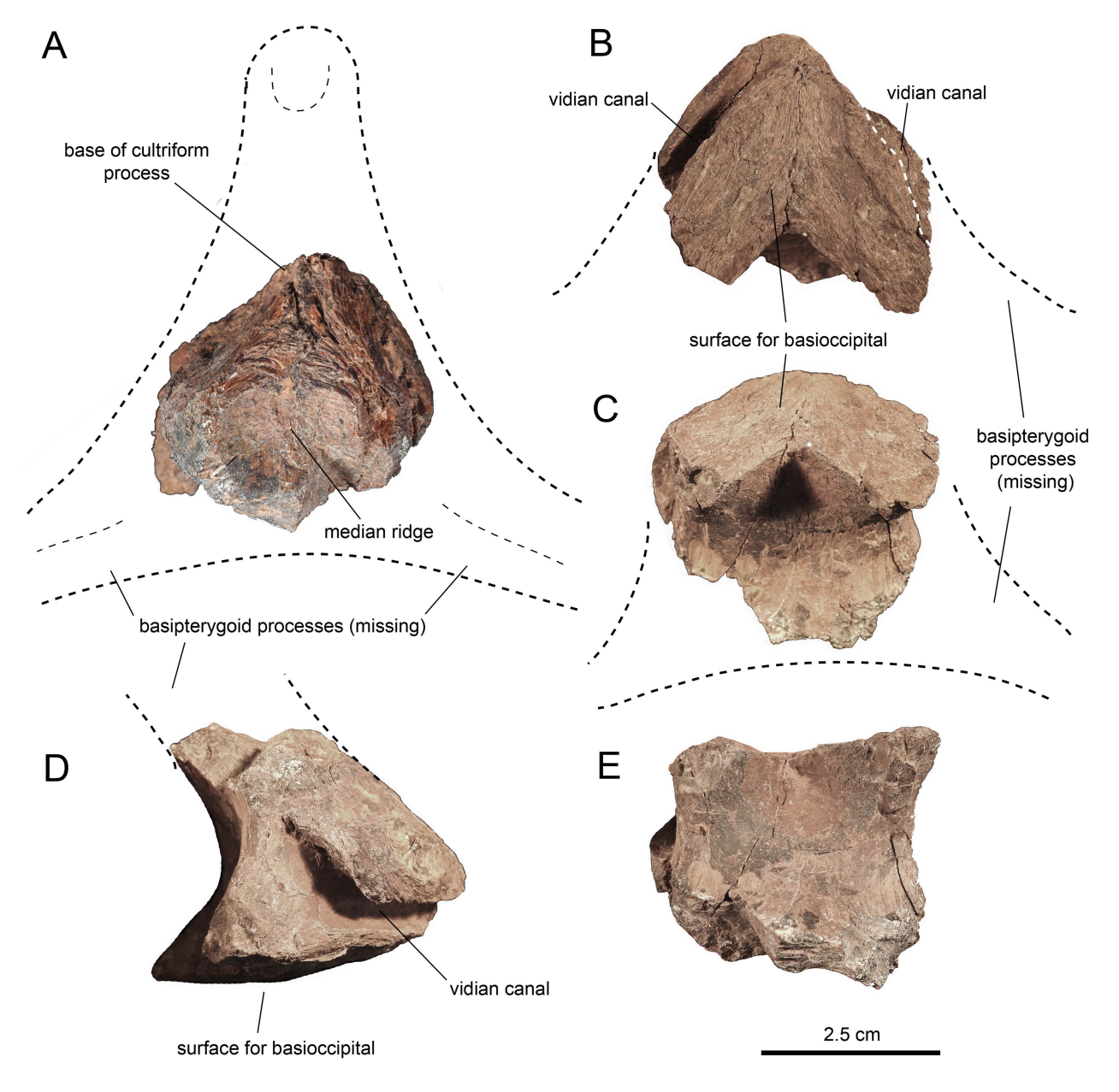
A
base of cultriform process
median ridge
basipterygoid processes (missing)
B
vidian canal
vidian canal
surface for basioccipital
C
basipterygoid processes (missing)
D
vidian canal
surface for basioccipital
E
2.5 cm

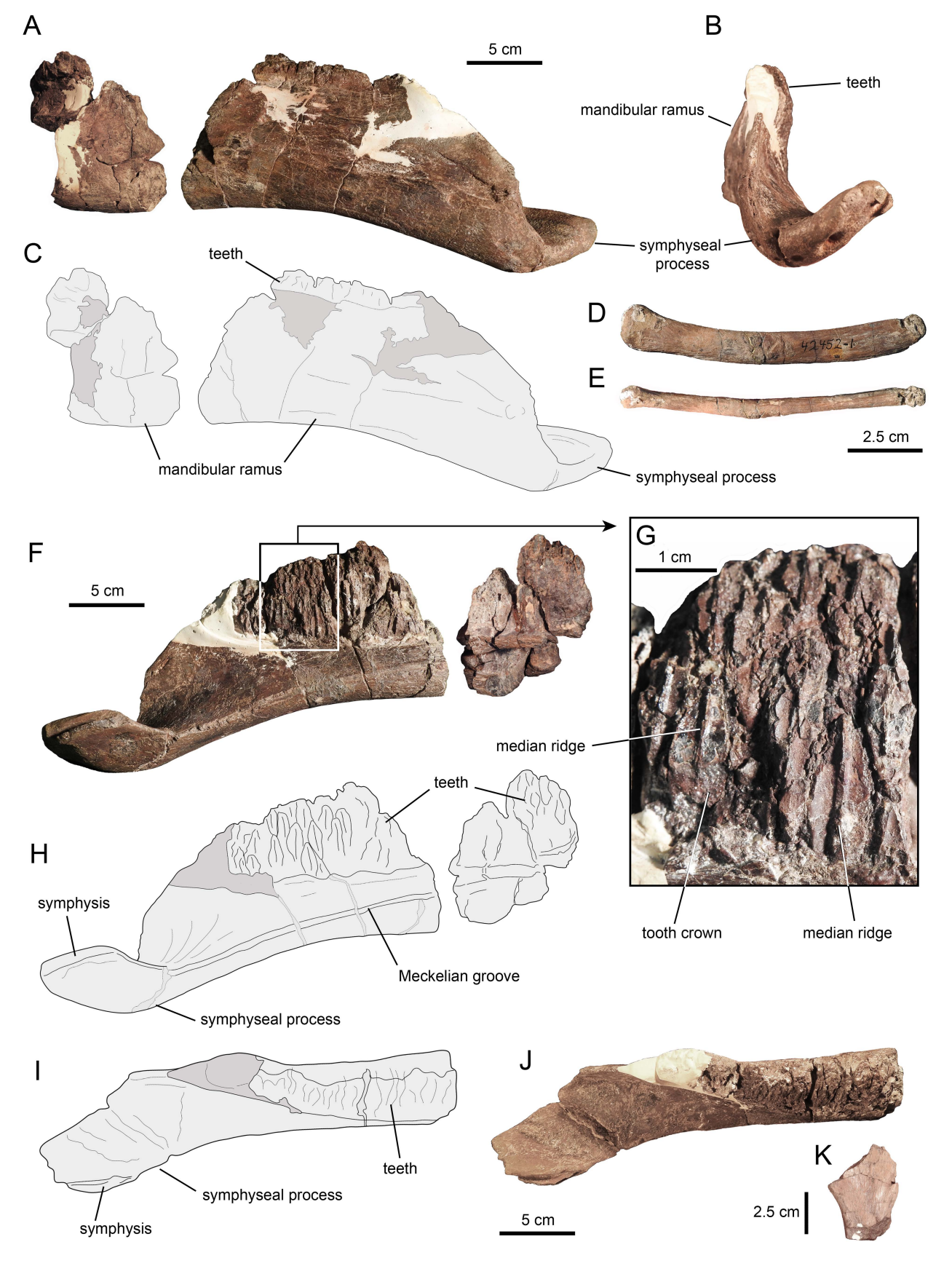
A
5 cm
B
teeth
mandibular ramus
symphyseal process
C
teeth
mandibular ramus
symphyseal process
D
42452-1
E
2.5 cm
F
5 cm
G
1 cm
median ridge
tooth crown
median ridge
H
teeth
symphysis
Meckelian groove
symphyseal process
I
teeth
symphyseal process
symphysis
J
5 cm
K
2.5 cm

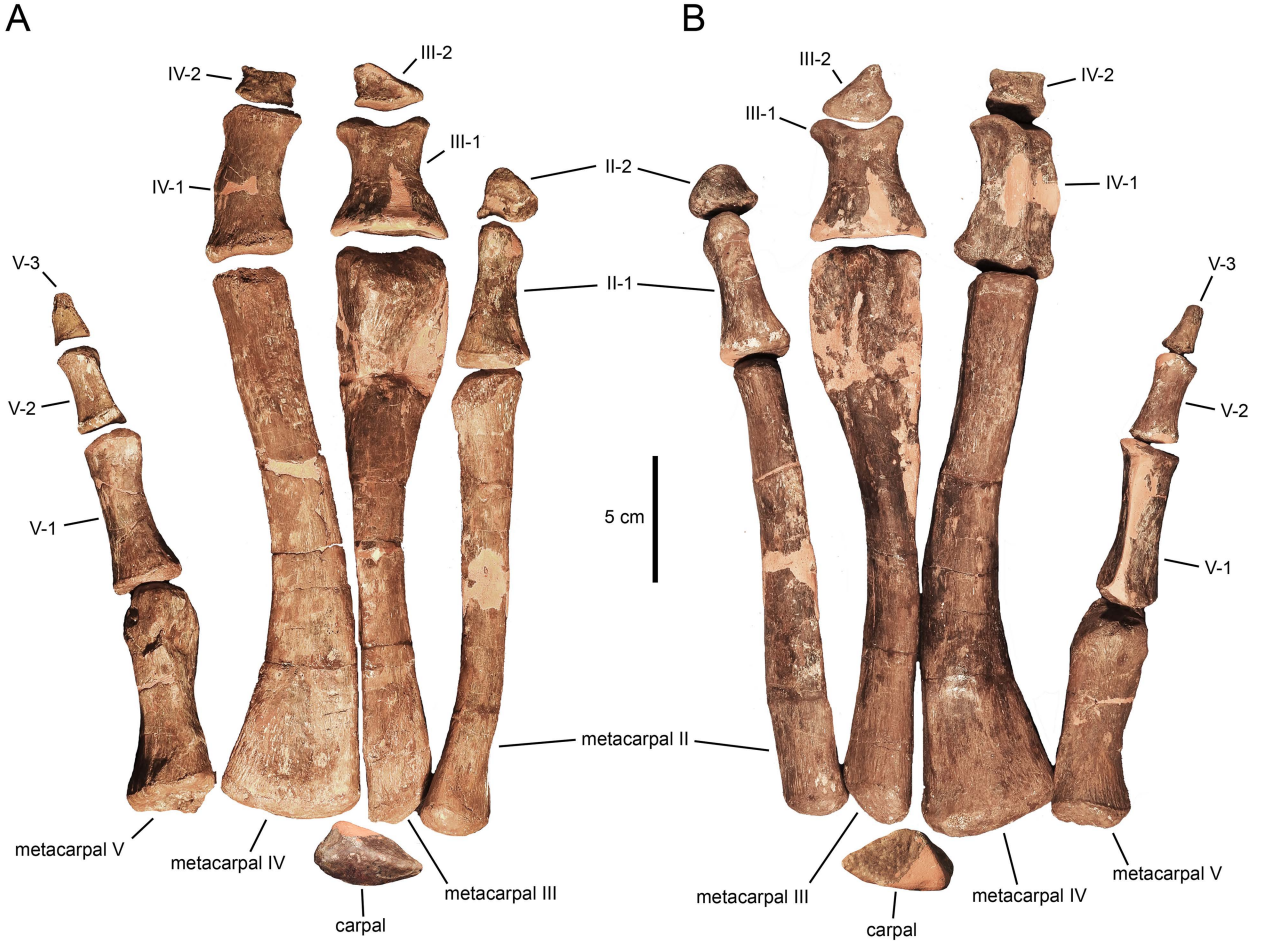
A
IV-2
III-2
III-1
IV-1
II-2
II-1
V-3
V-2
V-1
5 cm
metacarpal II
metacarpal V
metacarpal IV
metacarpal III
carpal
B
III-2
III-1
IV-2
IV-1
V-3
V-2
V-1
metacarpal III
carpal
metacarpal IV
metacarpal V

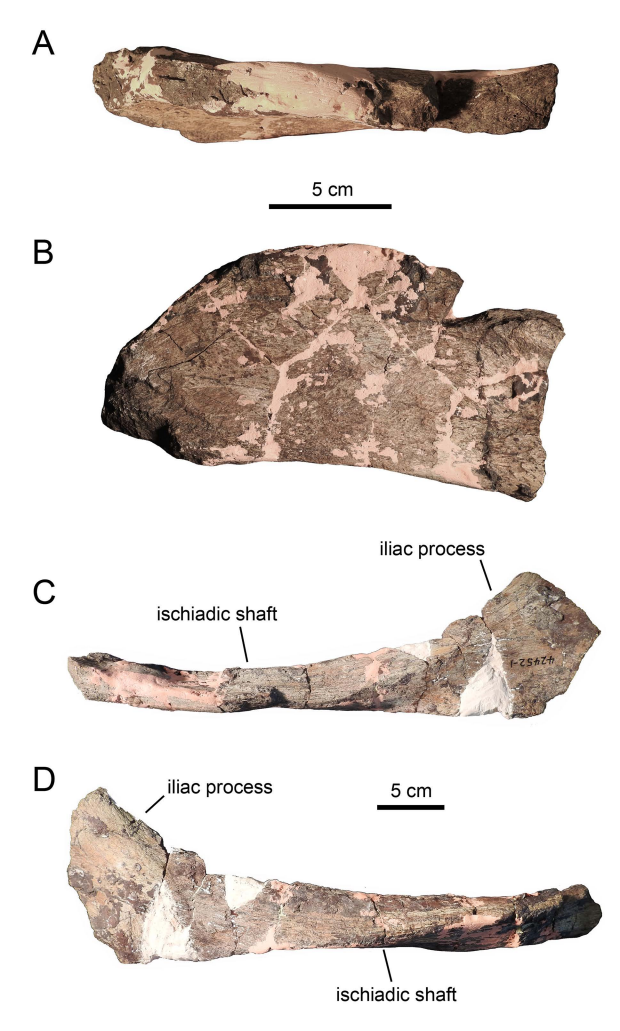
A
5 cm
B
iliac process
C
ischiadic shaft
42452-1
D
iliac process
5 cm
ischiadic shaft

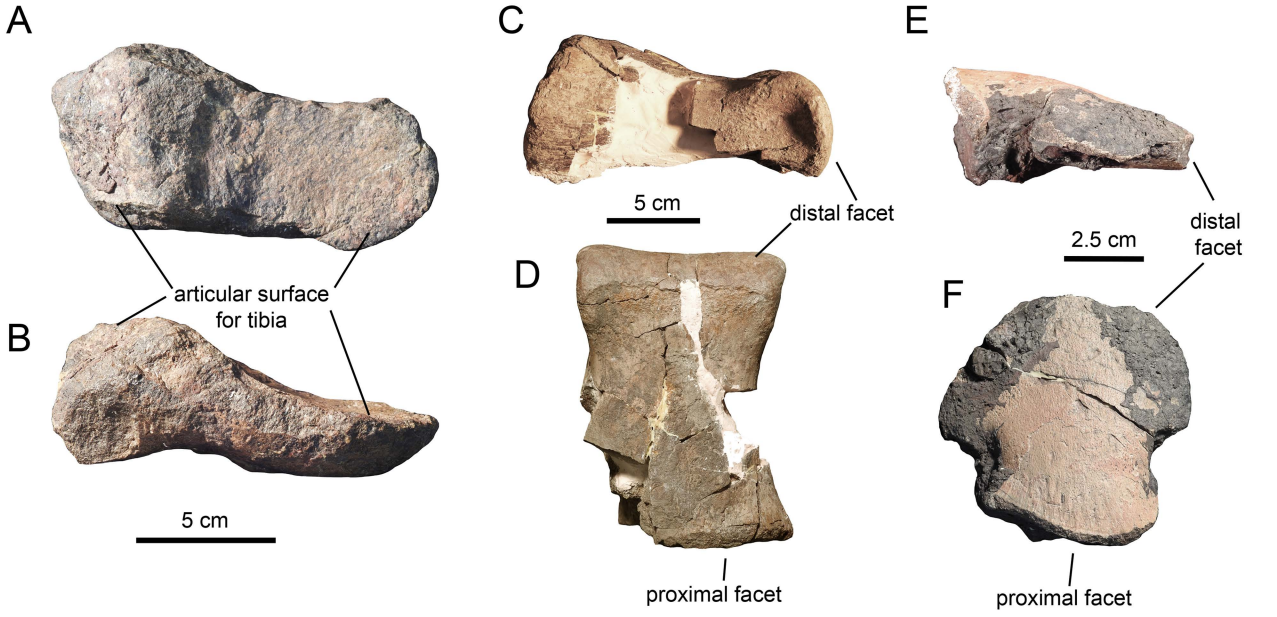
A
B
articular surface
for tibia
5 cm
C
5 cm
distal facet
D
proximal facet
E
2.5 cm
distal
facet
F
proximal facet

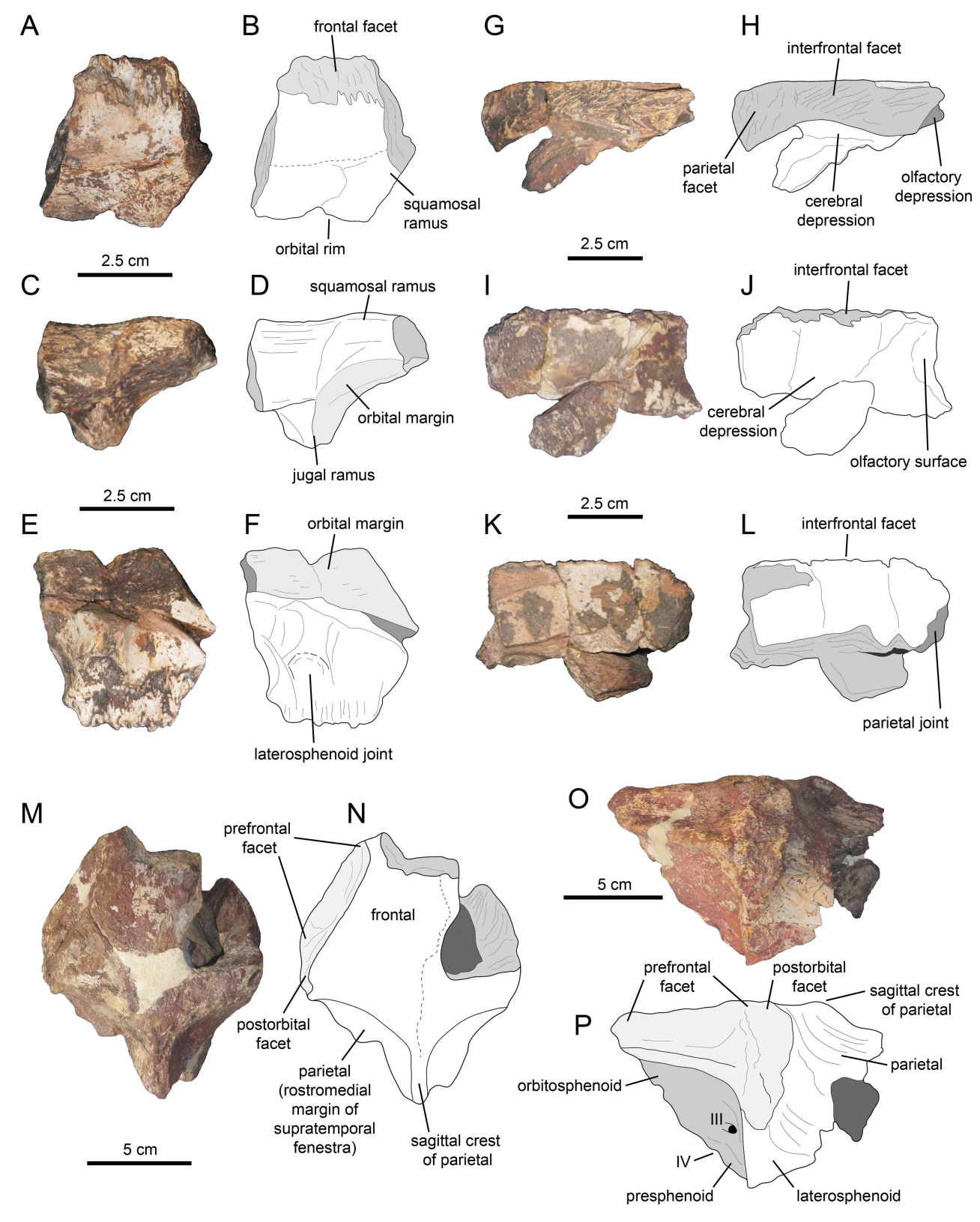
A
B
frontal facet
squamosal ramus
orbital rim
2.5 cm
G
H
interfrontal facet
parietal facet
cerebral depression
olfactory depression
2.5 cm
C
D
squamosal ramus
orbital margin
jugal ramus
2.5 cm
I
J
interfrontal facet
cerebral depression
olfactory surface
E
F
orbital margin
laterosphenoid joint
2.5 cm
K
L
interfrontal facet
parietal joint
M
5 cm
N
prefrontal facet
frontal
postorbital facet
parietal (rostromedial margin of supratemporal fenestra)
sagittal crest of parietal
O
5 cm
P
prefrontal facet
postorbital facet
sagittal crest of parietal
parietal
orbitosphenoid
III
IV
presphenoid
laterosphenoid

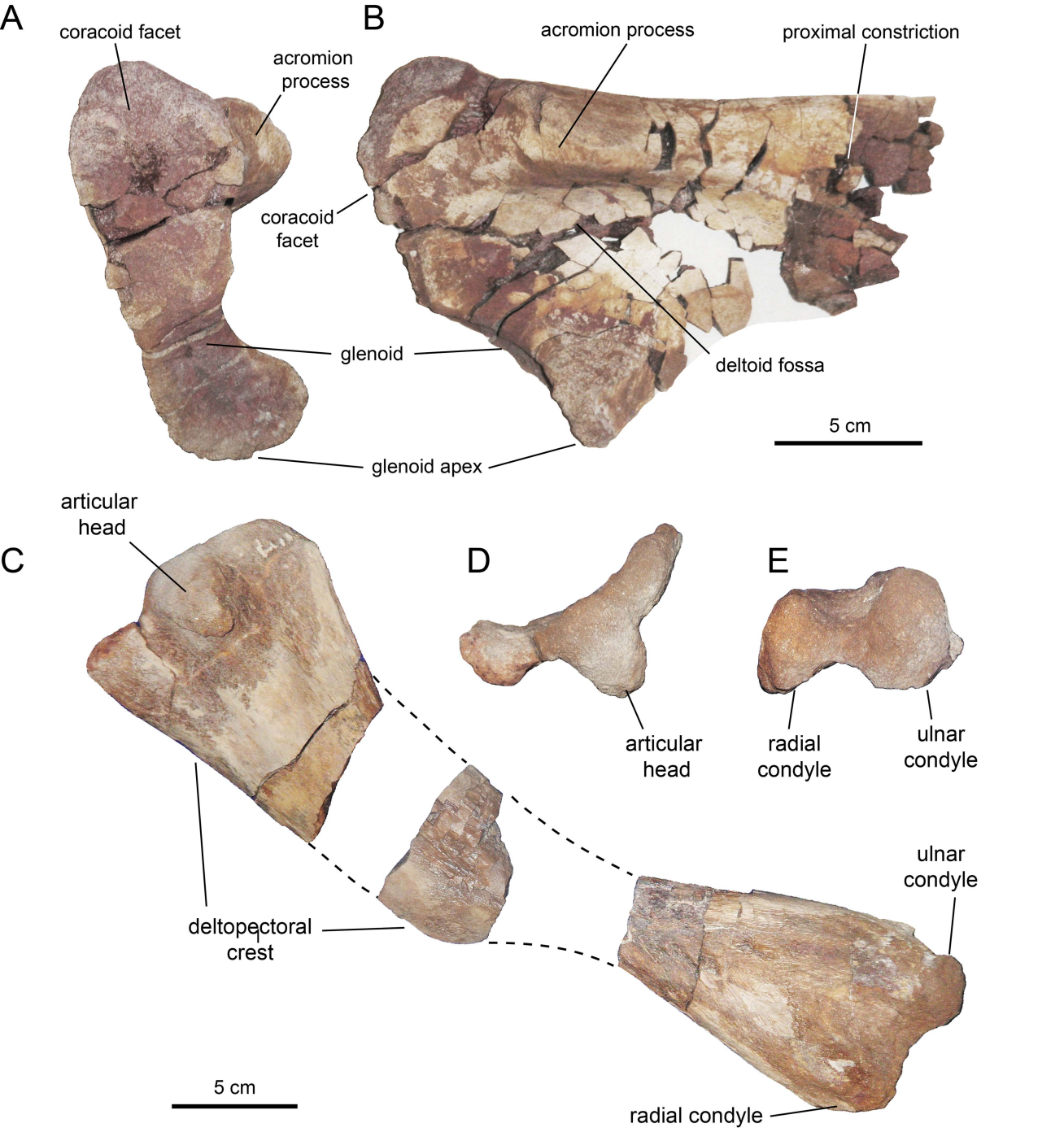
A
coracoid facet
acromion process
coracoid facet
glenoid
glenoid apex
B
acromion process
proximal constriction
deltoid fossa
5 cm
articular head
C
deltopectoral crest
5 cm
D
articular head
E
radial condyle
ulnar condyle
ulnar condyle
radial condyle

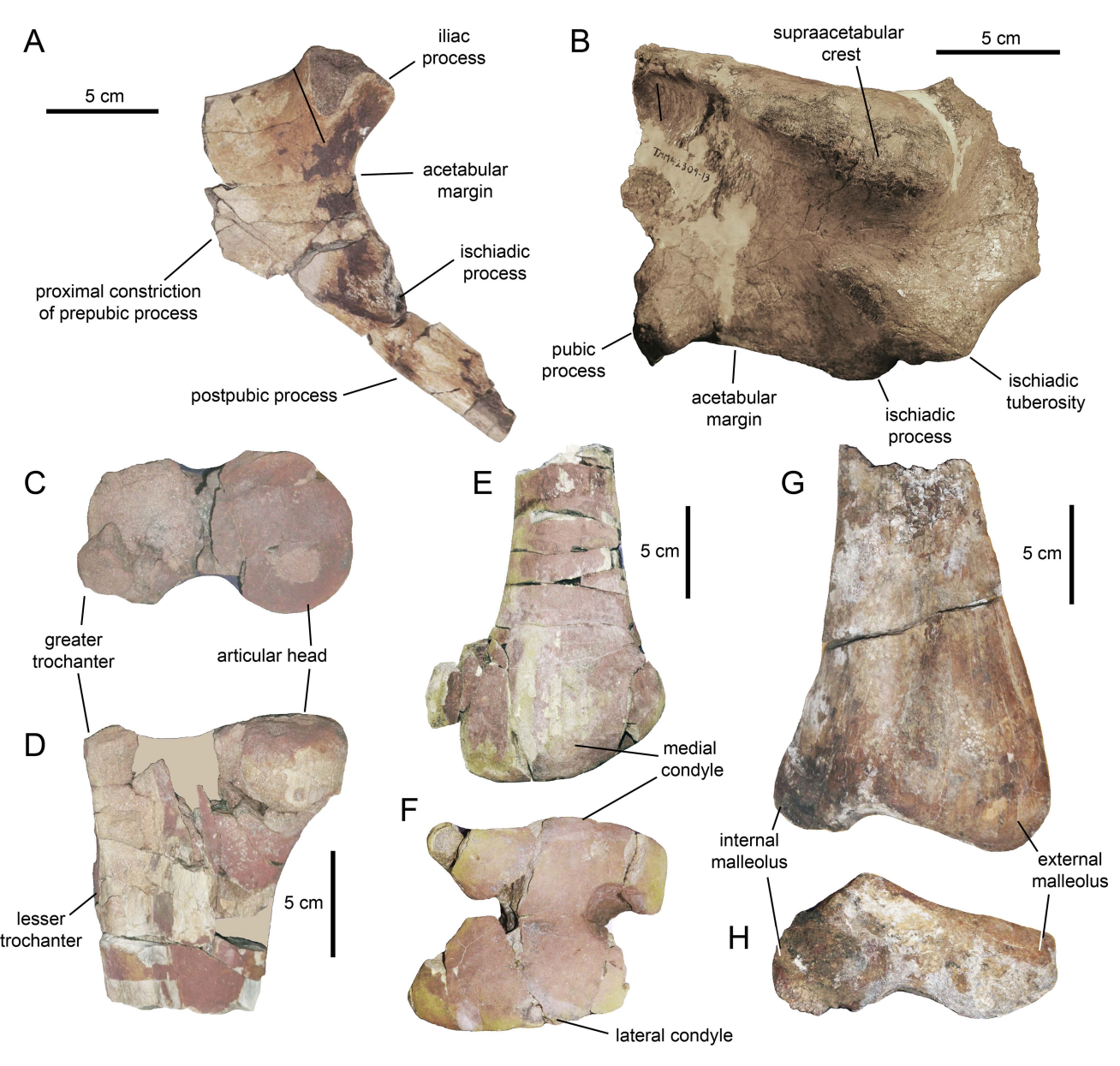
A
5 cm
iliac process
acetabular margin
ischiadic process
proximal constriction of prepubic process
postpubic process
B
supraacetabular crest
5 cm
pubic process
acetabular margin
ischiadic process
ischiadic tuberosity
C
greater trochanter
articular head
D
lesser trochanter
5 cm
E
5 cm
medial condyle
F
lateral condyle
G
5 cm
internal malleolus
external malleolus
H

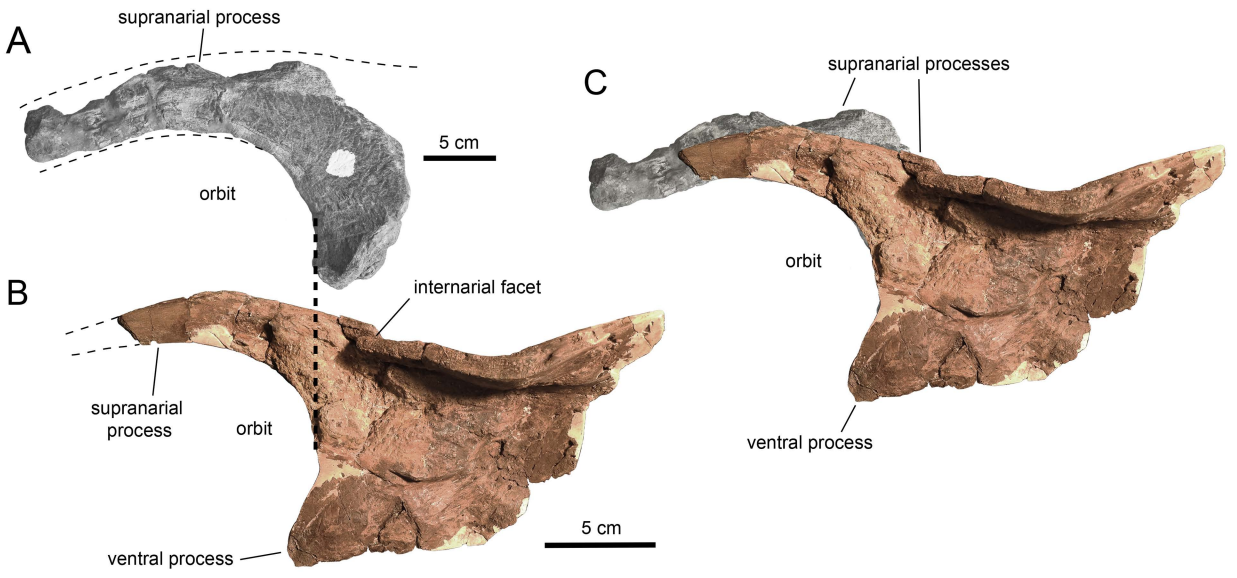
A
supranarial process
5 cm
orbit
B
internarial facet
supranarial process
orbit
5 cm
ventral process
C
supranarial processes
orbit
ventral process

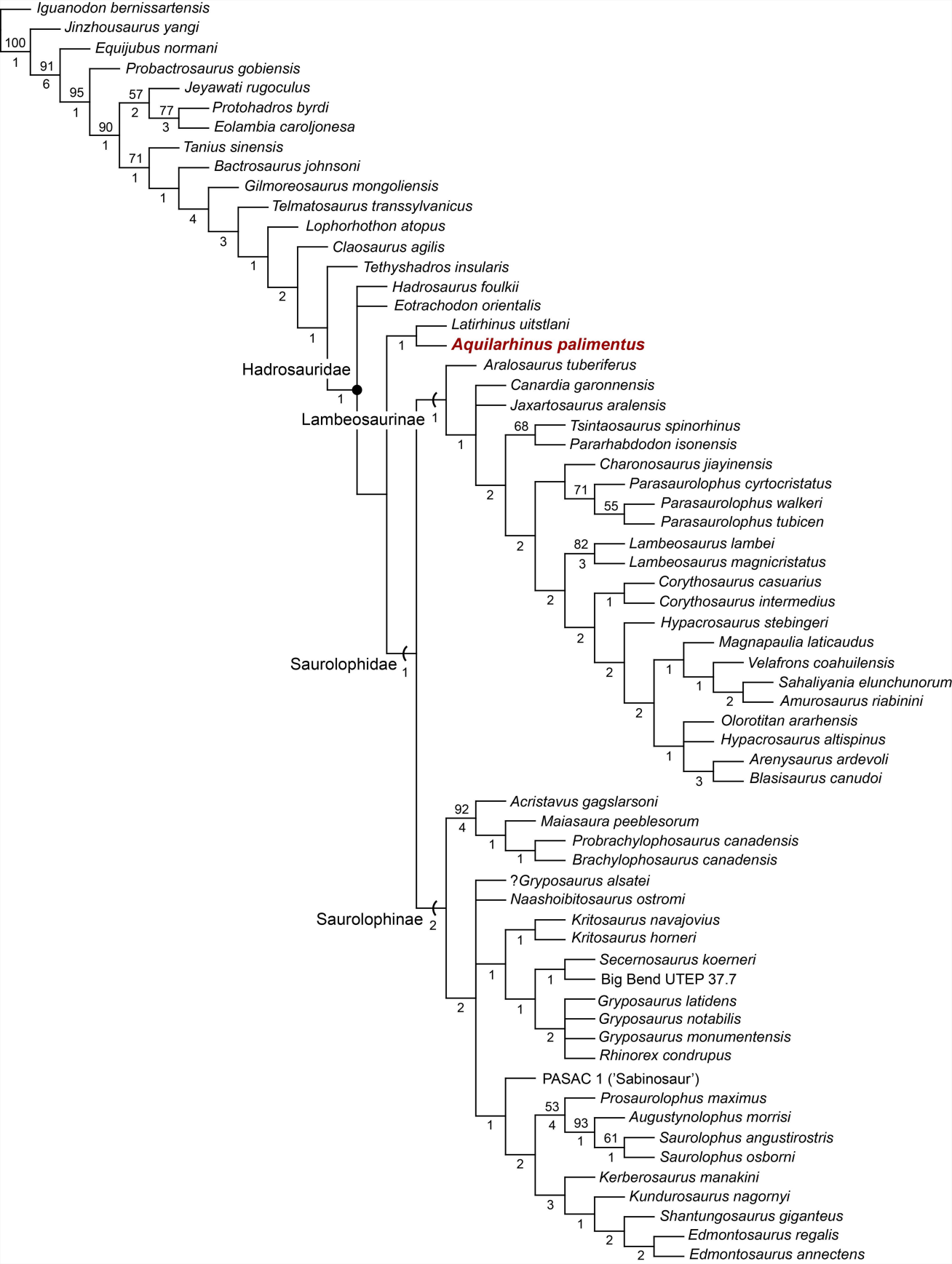
Iguanodon bernissartensis
Jinzhousaurus yangi
Equijubus normani
Probactrosaurus gobiensis
Jeyawati rugoculus
Protohadros byrdi
Eolambia caroljonesa
Tanius sinensis
Bactrosaurus johnsoni
Gilmoreosaurus mongoliensis
Telmatosaurus transsylvanicus
Lophorhothon atopus
Claosaurus agilis
Tethyshadros insularis
Hadrosaurus foulkii
Eotrachodon orientalis
Latirhinus uitstlani
Aquilarhinus palimentus
Hadrosauridae
Aralosaurus tuberiferus
Canardia garonnensis
Jaxartosaurus aralensis
Lambeosaurinae
Tsintaosaurus spinorhinus
Pararhabdodon isonensis
Charonosaurus jiayinensis
Parasaurolophus cyrtocristatus
Parasaurolophus walkeri
Parasaurolophus tubicen
Lambeosaurus lambei
Lambeosaurus magnicristatus
Corythosaurus casuarius
Corythosaurus intermedius
Hypacrosaurus stebingeri
Magnapaulia laticaudus
Velafrons coahuilensis
Sahaliyania elunchunorum
Amurosaurus riabinini
Olorotitan ararhensis
Hypacrosaurus altispinus
Arenysaurus ardevoli
Blasisaurus canudoi
Saurolophidae
Acristavus gagslarsoni
Maiasaura peeblesorum
Probrachylophosaurus canadensis
Brachylophosaurus canadensis
?Gryposaurus alsatei
Naashoibitosaurus ostromi
Saurolophinae
Kritosaurus navajovius
Kritosaurus horneri
Secernosaurus koerneri
Big Bend UTEP 37.7
Gryposaurus latidens
Gryposaurus notabilis
Gryposaurus monumentensis
Rhinorex condrupus
PASAC 1 ('Sabinosaur')
Prosaurolophus maximus
Augustynolophus morrisi
Saurolophus angustirostris
Saurolophus osborni
Kerberosaurus manakini
Kundurosaurus nagornyi
Shantungosaurus giganteus
Edmontosaurus regalis
Edmontosaurus annectens

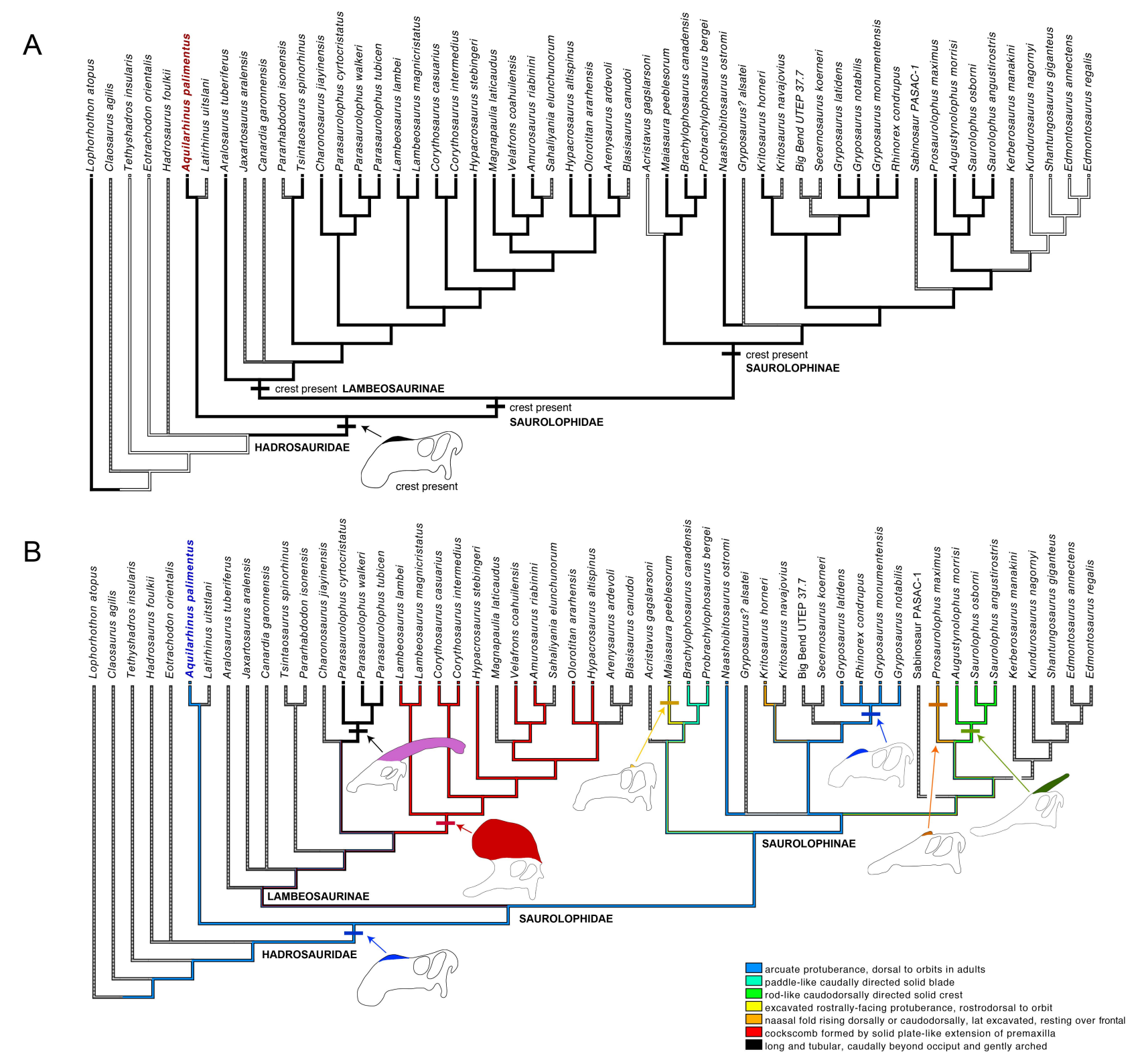
A
Lophorhothon atopus
Claosaurus agilis
Tethyshadros insularis
Eotrachodon orientalis
Hadrosaurus foulkii
Aquilarhinus palimentus
Latirhinus uitslani
Aralosaurus tuberiferus
Jaxartosaurus aralensis
Canardia garonnensis
Pararhabdodon isonensis
Tsintaosaurus spinorhinus
Charonosaurus jiayinensis
Parasaurolophus cyrtocristatus
Parasaurolophus walkeri
Parasaurolophus tubicen
Lambeosaurus lambei
Lambeosaurus magnicristatus
Corythosaurus casuarius
Corythosaurus intermedius
Hypacrosaurus stebingeri
Magnapaulia laticaudus
Velafrons coahuilensis
Amurosaurus riabinini
Sahaliyania elunchunorum
Hypacrosaurus altispinus
Olorotitan ararhensis
Arenysaurus ardevoli
Blasisaurus canudoi
Acristavus gagslarsoni
Maiasaura peeblesorum
Brachylophosaurus canadensis
Probrachylophosaurus bergei
Naashoibitosaurus ostromi
Gryposaurus? alsatei
Kritosaurus horneri
Kritosaurus navajovius
Big Bend UTEP 37.7
Secernosaurus koerneri
Gryposaurus latidens
Gryposaurus notabilis
Gryposaurus monumentensis
Rhinorex condrupus
Sabinosaur PASAC-1
Prosaurolophus maximus
Augustynolophus morrisi
Saurolophus osborni
Saurolophus angustirostris
Kerberosaurus manakini
Kundurosaurus nagornyi
Shantungosaurus giganteus
Edmontosaurus annectens
Edmontosaurus regalis
crest present
SAUROLOPHINAE
crest present LAMBEOSAURINAE
crest present
SAUROLOPHIDAE
HADROSAURIDAE
crest present
B
SAUROLOPHINAE
LAMBEOSAURINAE
SAUROLOPHIDAE
HADROSAURIDAE
arcuate protuberance, dorsal to orbits in adults
paddle-like caudally directed solid blade
rod-like caudodorsally directed solid crest
excavated rostrally-facing protuberance, rostrodorsal to orbit
naasal fold rising dorsally or caudodorsally, lat excavated, resting over frontal
cockscomb formed by solid plate-like extension of premaxilla
long and tubular, caudally beyond occiput and gently arched

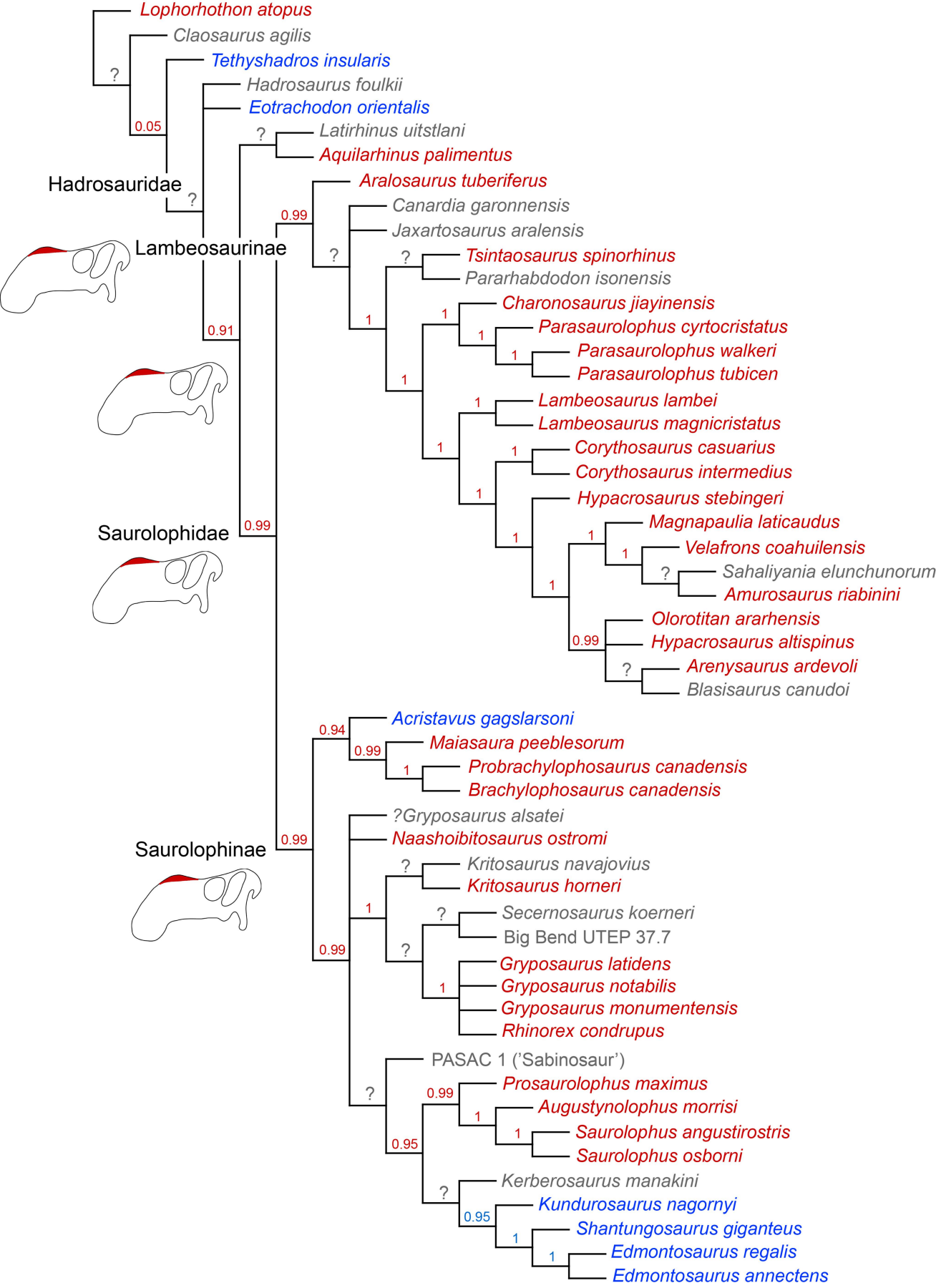
Lophorhothon atopus
Claosaurus agilis
Tethyshadros insularis
Hadrosaurus foulkii
Eotrachodon orientalis
Latirhinus uitstlani
Aquilarhinus palimentus
Hadrosauridae
Aralosaurus tuberiferus
Canardia garonnensis
Jaxartosaurus aralensis
Lambeosaurinae
Tsintaosaurus spinorhinus
Pararhabdodon isonensis
Charonosaurus jiayinensis
Parasaurolophus cyrtocristatus
Parasaurolophus walkeri
Parasaurolophus tubicen
Lambeosaurus lambei
Lambeosaurus magnicristatus
Corythosaurus casuarius
Corythosaurus intermedius
Hypacrosaurus stebingeri
Magnapaulia laticaudus
Velafrons coahuilensis
Sahaliyania elunchunorum
Amurosaurus riabinini
Olorotitan ararhensis
Hypacrosaurus altispinus
Arenysaurus ardevoli
Blasisaurus canudoi
Saurolophidae
Acristavus gagslarsoni
Maiasaura peeblesorum
Probrachylophosaurus canadensis
Brachylophosaurus canadensis
?Gryposaurus alsatei
Naashoibitosaurus ostromi
Kritosaurus navajovius
Kritosaurus horneri
Secernosaurus koerneri
Big Bend UTEP 37.7
Gryposaurus latidens
Gryposaurus notabilis
Gryposaurus monumentensis
Rhinorex condrupus
Saurolophinae
PASAC 1 ('Sabinosaur')
Prosaurolophus maximus
Augustynolophus morrisi
Saurolophus angustirostris
Saurolophus osborni
Kerberosaurus manakini
Kundurosaurus nagornyi
Shantungosaurus giganteus
Edmontosaurus regalis
Edmontosaurus annectens

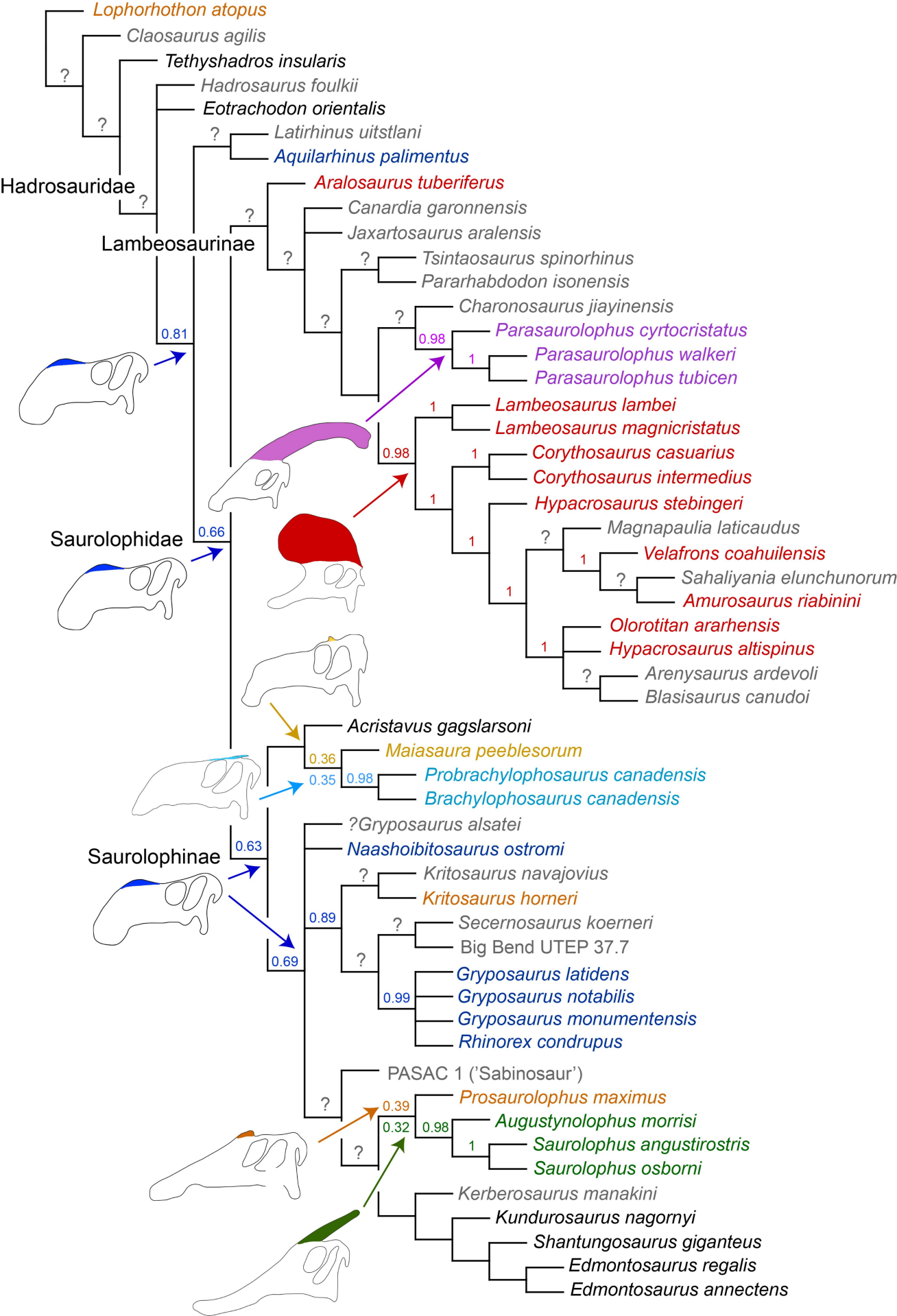
Lophorhothon atopus
Claosaurus agilis
Tethyshadros insularis
Hadrosaurus foulkii
Eotrachodon orientalis
Latirhinus uitstlani
Aquilarhinus palimentus
Hadrosauridae
Aralosaurus tuberiferus
Canardia garonnensis
Jaxartosaurus aralensis
Lambeosaurinae
Tsintaosaurus spinorhinus
Pararhabdodon isonensis
Charonosaurus jiayinensis
Parasaurolophus cyrtocristatus
Parasaurolophus walkeri
Parasaurolophus tubicen
Lambeosaurus lambei
Lambeosaurus magnicristatus
Corythosaurus casuarius
Corythosaurus intermedius
Hypacrosaurus stebingeri
Magnapaulia laticaudus
Velafrons coahuilensis
Sahaliyania elunchunorum
Amurosaurus riabinini
Olorotitan ararhensis
Hypacrosaurus altispinus
Arenysaurus ardevoli
Blasisaurus canudoi
Saurolophidae
Acristavus gagslarsoni
Maiasaura peeblesorum
Probrachylophosaurus canadensis
Brachylophosaurus canadensis
?Gryposaurus alsatei
Naashoibitosaurus ostromi
Saurolophinae
Kritosaurus navajovius
Kritosaurus horneri
Secernosaurus koerneri
Big Bend UTEP 37.7
Gryposaurus latidens
Gryposaurus notabilis
Gryposaurus monumentensis
Rhinorex condrupus
PASAC 1 ('Sabinosaur')
Prosaurolophus maximus
Augustynolophus morrisi
Saurolophus angustirostris
Saurolophus osborni
Kerberosaurus manakini
Kundurosaurus nagornyi
Shantungosaurus giganteus
Edmontosaurus regalis
Edmontosaurus annectens
0.81
0.66
0.63
0.69
0.98
1
0.36
0.35
0.98
0.89
0.99
0.39
0.32
0.98
1